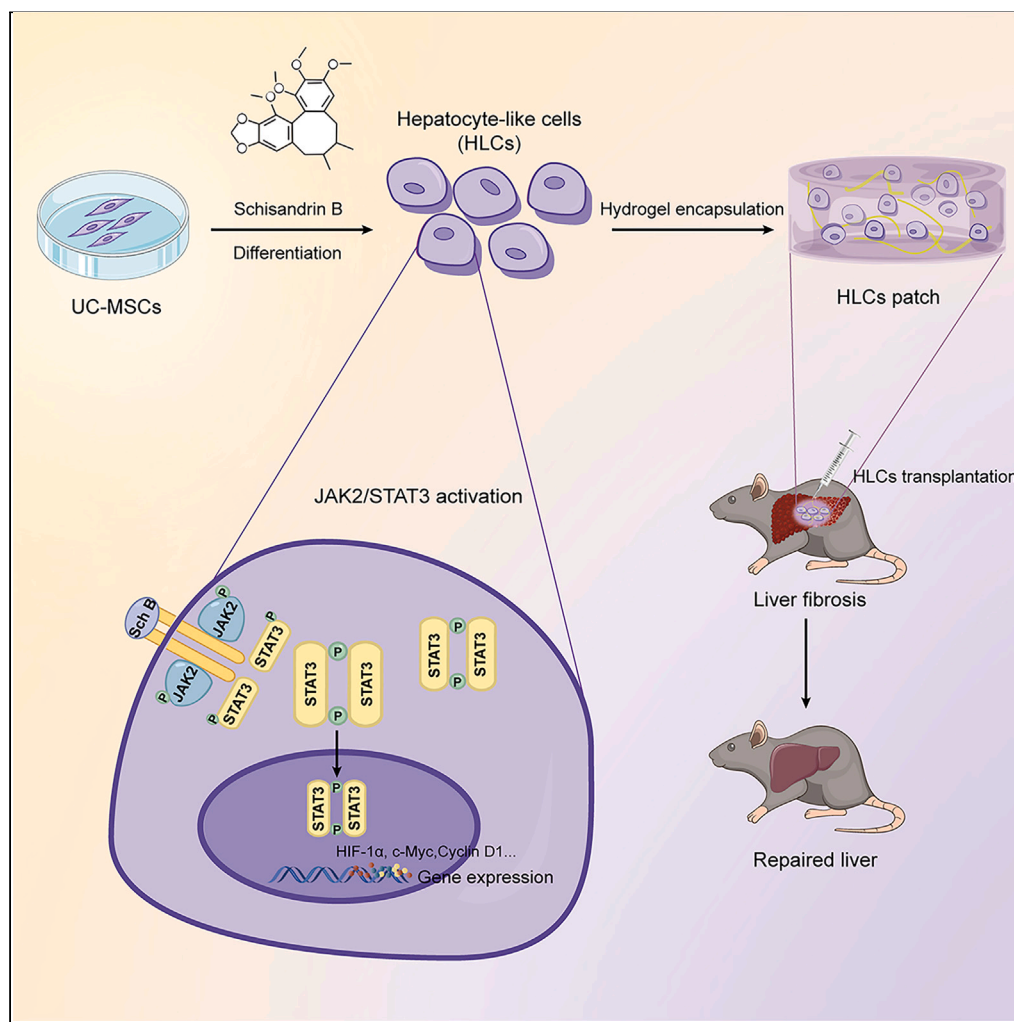


Article

# Schisandrin B promotes hepatic differentiation from human umbilical cord mesenchymal stem cells



Meixian Jin, Xiao Yi, Xiaojuan Zhu, ..., Shiyuan Xu, Ying Zhang, Shuqin Zhou

xsy998@smu.edu.cn (S.X.)  
yingzhang0831@163.com (Y.Z.)  
zhoushuqin@smu.edu.cn (S.Z.)

**Highlights**

Schisandrin B enhances the hepatic differentiation and maturation of UC-MSCs

Schisandrin B promotes hepatic differentiation via activation of JAK2/STAT3 pathway

Schisandrin B-treated hepatocyte-like cells alleviate liver fibrosis in mice



## Article

## Schisandrin B promotes hepatic differentiation from human umbilical cord mesenchymal stem cells

Meixian Jin,<sup>1,6</sup> Xiao Yi,<sup>2,6</sup> Xiaojuan Zhu,<sup>3</sup> Wei Hu,<sup>1</sup> Simin Wang,<sup>1</sup> Qi Chen,<sup>1</sup> Wanren Yang,<sup>4</sup> Yang Li,<sup>4</sup> Shao Li,<sup>4</sup> Qing Peng,<sup>4</sup> Mingxin Pan,<sup>4</sup> Yi Gao,<sup>4</sup> Shiyuan Xu,<sup>1,\*</sup> Ying Zhang,<sup>4,\*</sup> and Shuqin Zhou<sup>1,5,7,\*</sup>

## SUMMARY

**Human umbilical cord mesenchymal stem cells (UC-MSCs)-derived hepatocyte-like cells (HLCs) have shown great promise in the treatment of liver diseases. However, most current induction protocols yield hepatocyte-like cells with limited function as compared with primary hepatocytes. Schisandrin B (Sch B) is one of the main components of *Schisandra chinensis*, which can prevent fibrosis progression and promote liver cell regeneration. Herein, we investigated the effects of Sch B on hepatic differentiation of UC-MSCs. We found that treatment with 10  $\mu$ M Sch B from the second stage of the differentiation process increased hepatic marker levels and hepatic function. Additionally, RNA-seq analysis revealed that Sch B promoted hepatic differentiation via activating the JAK2/STAT3 pathway. When transplanted HLCs into mice with CCL<sub>4</sub>-induced liver fibrosis, Sch B-treated HLCs exhibited significant therapeutic effects. This study provides an optimized hepatic differentiation protocol for UC-MSCs based on Sch B, yielding functioning cells for liver disease treatment.**

## INTRODUCTION

Liver is one of the most important organs in the human body, with complex functions. Liver disease can be caused by a variety of factors (viral, drug and alcohol abuse, metabolic, genetic, cancer, or immune), and liver damage from these causes can progress to severe liver failure.<sup>1</sup> Liver transplantation remains the most effective treatment for end-stage liver disease. However, liver transplantation is limited because of the severe shortage of liver donors, immune reaction and high mortality.<sup>2</sup> An artificial liver support system, the cell-based bioartificial liver, has been used as an alternative or transitional treatment before transplantation. The cell-based bioartificial liver can not only remove metabolic wastes and toxins but also provide important liver functions including metabolite synthesis and biotransformation, which is an ideal therapeutic model for artificial liver.<sup>3</sup> In addition, hepatocyte transplantation has been considered a feasible alternative therapy. In fact, achieving the ideal therapeutic goal of a bioartificial liver or hepatocyte transplantation relies on large-scale functional hepatocytes. However, the use of primary hepatocytes is limited because of the inconvenience of extraction, challenges in expansion, and short cell life span *in vitro*.<sup>4</sup> How to obtain a large number of functional hepatocytes remains a key issue. With the development of stem cell technology, researchers have focused more on stem cells, characterized by their self-renewable ability, high proliferative potential, multipotent competences and abundant source. Stem cells can differentiate into a variety of cells, including hepatocytes, thus bringing new hope for treating liver diseases.<sup>5</sup>

Various stem cells are able to differentiate into hepatocyte-like cells (HLCs). As compared with embryonic stem cells and induced pluripotent stem cells, mesenchymal stem cells (MSCs) have the advantages of abundant source, low immunogenicity, and fewer ethical issues.<sup>6</sup> Currently, MSCs are being widely used for the treatment of various diseases such as cardiovascular diseases, metabolic disorders, neurodegenerative and neurodevelopmental disorders, wound healing, eyesight diseases, bone regeneration, periodontal regeneration, and various autoimmune diseases.<sup>7,8</sup> The therapeutic potential of MSCs is based on two main aspects: their ability to differentiate into different cell lines to replace damaged tissue, and their ability to regulate the immune response through paracrine effects.<sup>9</sup> The primary sources of MSCs used for disease treatment are the umbilical cord and bone marrow. Compared to bone marrow mesenchymal stem cells (BM-MSCs), umbilical cord mesenchymal stem cells (UC-MSCs) have higher proliferation and hepatic differentiation ability, and lower immunogenicity.<sup>10</sup> Therefore,

<sup>1</sup>Department of Anesthesiology, Zhujiang Hospital, Southern Medical University, Guangzhou 510000, China

<sup>2</sup>Department of Gynecology, Zhujiang Hospital, Southern Medical University, Guangzhou 510000, China

<sup>3</sup>Department of Anesthesiology, First People's Hospital of Kashi, Kashi 844000, China

<sup>4</sup>General Surgery Center, Department of Hepatobiliary Surgery II, Guangdong Provincial Research Center for Artificial Organ and Tissue Engineering, Guangdong Provincial Key Laboratory of Viral Hepatitis Research, Institute of Regenerative Medicine, Zhujiang Hospital, Southern Medical University, Guangzhou 510000, China

<sup>5</sup>Anesthesiology Department of The Second Affiliated Hospital, School of Medicine, The Chinese University of Hong Kong, Shenzhen & Longgang District People's Hospital of Shenzhen, Shenzhen 518172, China

<sup>6</sup>These authors contributed equally

<sup>7</sup>Lead contact

\*Correspondence: xsy998@smu.edu.cn (S.X.), yingzhang0831@163.com (Y.Z.), zhoushuqin@smu.edu.cn (S.Z.)

<https://doi.org/10.1016/j.isci.2024.108912>



UC-MSCs are considered an ideal source of hepatocytes for transplantation. MSCs-derived HLCs can replace injured hepatocytes *in vivo* and restore liver functions. There are many methods of inducing UC-MSCs into HLCs *in vitro*.<sup>11</sup> However, most current induction protocols yield HLCs that are not sufficiently functional to achieve the desired therapeutic effect.<sup>12,13</sup> Therefore, we need to improve the efficiency of hepatic differentiation of stem cells in the application of stem cells.

Traditional Chinese medicine plays an important role in the treatment of diseases. In recent years, extracts or compounds from some traditional Chinese medicine, such as salviolic acid B, fuzheng huayu, and salidroside, have been shown to enhance the differentiation of stem cells into hepatocytes.<sup>14–16</sup> *S. chinensis* is a widely used hepato-protective herb in the clinic; it can reduce oxidative stress, improve liver function, and facilitate hepatocyte proliferation and liver regeneration.<sup>17–19</sup> Schisandrin B (Sch B) is a monomer extracted from *S. chinensis*. Sch B possesses a wide range of biological properties and plays an essential role in liver protection, anti-oxidation, anti-inflammation, anti-tumor, neuroprotection, and cardioprotection.<sup>20</sup> Studies have reported that Sch B can effectively prevent cell apoptosis, slow down fibrosis progression, induce cytochrome P450 (CYP) enzyme activity, and promote liver regeneration.<sup>21–23</sup> In addition, several studies have demonstrated that Sch B can inhibit the growth of various types of cancers, including lung cancer, cholangiocarcinoma, gastric cancer, melanoma, and glioma, by inducing cell-cycle arrest or apoptosis.<sup>20</sup> Sch B alleviates myocardial ischemia-reperfusion injury,<sup>24</sup> drug-induced hepatotoxicity<sup>25</sup> and nephrotoxicity<sup>26</sup> by reducing oxidative stress and apoptosis. A study has shown that it enhances neural stem cell proliferation and promotes nerve formation as well as neural differentiation.<sup>27</sup> However, whether it can enhance the hepatic differentiation of stem cells is unclear. *S. chinensis* is one of the components of the traditional Chinese medicine compound fuzheng huayu, which has been found to promote the hepatic differentiation of stem cells as described above. Therefore, we hypothesized that Sch B treatment might help enhance the hepatic differentiation of UC-MSCs.

In this study, we investigated the effect of Sch B on the hepatic differentiation of UC-MSCs and found that Sch B enhanced their hepatic differentiation. Furthermore, RNA-seq was used to identify the potential mechanism of Sch B on UC-MSCs differentiation. Sch B promoted hepatic differentiation via activating the JAK2/STAT3 pathway. And the effectiveness of HLCs in treating chronic liver disease was evaluated *in vivo* by using a CCL<sub>4</sub>-induced liver fibrosis mouse mode. This protocol offers an optimized hepatic differentiation protocol for UC-MSCs, providing an alternative source of hepatocytes for liver disease treatment.

## RESULTS

### Isolation and identification of UC-MSCs

UC-MSCs were isolated as in our previous study by using a tissue explant procedure. Cells migrating from the tissue displayed a fibroblastoid morphology 7 days after seeding in growth medium (Figure 1A); Cells approached 80% confluence at 14 days (Figure 1B). These cells were harvested and proliferated for further use.

Immunophenotyping of cells by flow cytometry revealed a positive expression of CD105 (98.94%), CD73 (99.77%), and CD90 (99.83%) markers on their surface, with lower expression of CD34, CD14, and HLA-DR markers (<2%) (Figure 1C). On Oil red O staining, adipogenic-induced UC-MSCs showed lipid vesicle accumulation (Figure 1D). Osteogenic-induced UC-MSCs exhibited calcium deposition and stained positive with alizarin red (Figure 1D). The neurogenically differentiated UC-MSCs showed extensive accumulation of Nissl bodies stained dark black-violet (Figure 1D). Undifferentiated cells showed negative staining. These results met the minimum standards of the International Society for Cell Therapy.<sup>28</sup>

### Determining the optimal concentration and treatment time of Sch B

Sch B had dose-dependent toxic effects on UC-MSCs (Figure 2A). Treatment with 0–25  $\mu$ M Sch B resulted in high cell viability (mean > 89.82  $\pm$  3.53%), but at > 25  $\mu$ M, cell viability decreased significantly. With 50  $\mu$ M Sch B, the mean cell viability was only 8.72  $\pm$  0.72%. Therefore, 0–25  $\mu$ M was safe for UC-MSCs. Furthermore, the 50% inhibitory concentration of Sch B was calculated as 32.91  $\mu$ M. Two safe concentrations (5  $\mu$ M and 10  $\mu$ M) were employed for the subsequent experiments.

To investigate the optimal treatment time, 5  $\mu$ M and 10  $\mu$ M Sch B was added at different stages of induction. The addition of Sch B resulted in higher mRNA levels of ALB, CYP3A4, CYP1A2, CYP2E1, and CYP2C9 compared to the control group (Figure 2C). This suggests that Sch B has the potential to enhance the differentiation of UC-MSCs into HLCs. Furthermore, a comparison of the two concentrations of Sch B revealed that the mRNA levels were higher with 10  $\mu$ M treatment compared to 5  $\mu$ M. Notably, the highest mRNA level was observed when Sch B treatment was initiated from the second stage. This preliminary experiment suggested that 10  $\mu$ M Sch B applied at the second stage of UC-MSCs hepatic differentiation was optimal.

During the differentiation process, the cell morphology underwent a gradual transition from spindle-shaped to polygonal-shaped, aligning with the typical characteristics of HLCs. These morphological changes were first observed at the second stage of the induction process. Additionally, there were similar morphology changes between the two groups (Figure 2D). The optimized differentiation protocol with Sch B is illustrated in Figure 2B.

### Enhancement of hepatocyte differentiation and maturation by Sch B

After determining the optimal concentration and treatment time of Sch B, we further explored the effect of Sch B on the hepatic differentiation of UC-MSCs. The mRNA expression of several stemness markers such as OCT-4, Nanog and Sox2 was decreased after induction (Figure 3A),

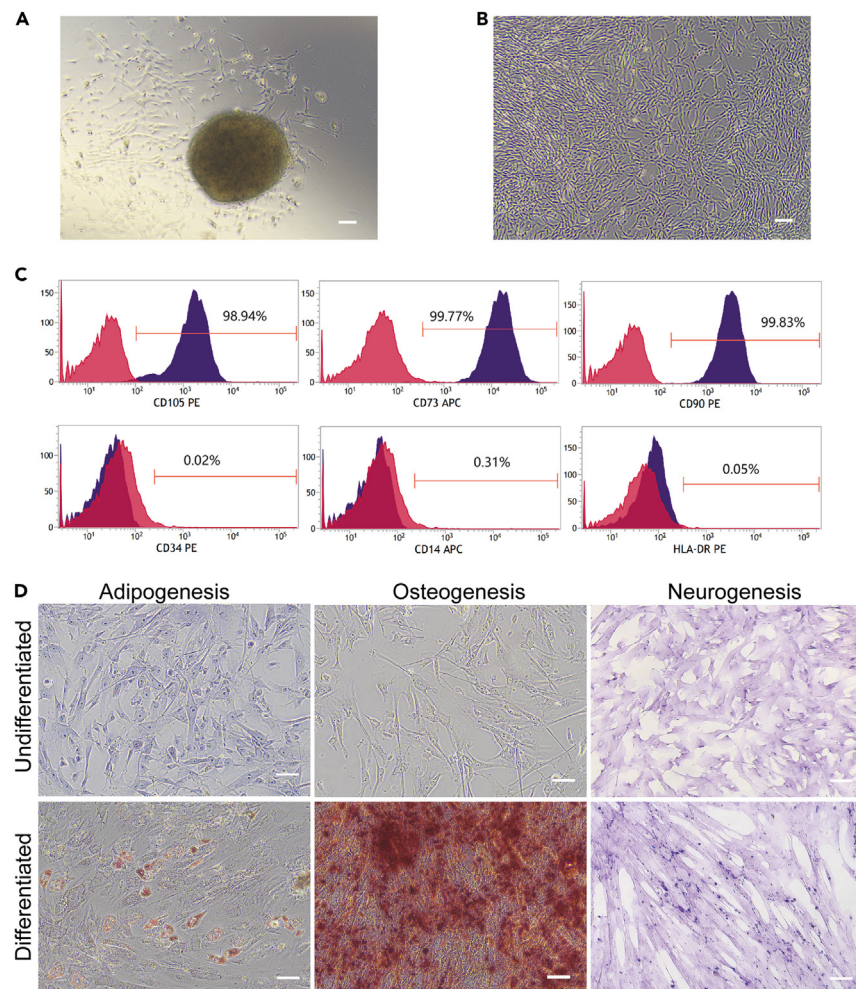


**Figure 1. Isolation and identification of umbilical cord mesenchymal stem cells (UC-MSCs)**

(A) Microscopy images of primary UC-MSCs migrating from umbilical cord tissue at 7 days. Scale bar = 100  $\mu$ m.

(B) UC-MSCs at 80% confluence. Scale bar = 100  $\mu$ m.

(C) Flow cytometry of the expression of surface markers on UC-MSCs.

(D) Multiple differentiation potential of UC-MSCs. Scale bar = 100  $\mu$ m.

so treatment with Sch B decreased the stemness characteristic in the HLCs. The expression of AFP (a marker of fetal hepatocytes) did not differ between groups with or without Sch B.

Metabolic function is one of the most important actions of hepatocytes, with the phase I metabolizing enzyme CYP playing a key role. The expression of phase I metabolizing enzyme genes CYP3A4, CYP1A2, CYP2E1, and CYP2D6 increased after Sch B treatment (Figure 3A). The expression of mature hepatocyte marker ALB increased by 2.5-fold and that of CYP3A4 by 6.5-fold. As compared with HLCs without Sch B treatment, Sch B-treated cells showed significantly increased expression of hepatocyte mature markers and liver function-related genes (Figure 3A). In addition, we observed that Sch B-treated cells displayed higher levels of hepatic markers compared to the two reported traditional Chinese medicine monomers (Salvianolic acid B and Salidroside) (Figure S1).

On immunofluorescence analysis, both groups of HLCs induced with and without Sch B exhibited elevated labeling for hepatic markers such as ALB, CK18, and CYP3A4 in comparison to undifferentiated UC-MSCs (Figure 3B). Further quantification of fluorescence displayed that the expression of ALB, CK18, and CYP3A4 in HLCs treated with Sch B was 2.3, 1.5, and 3.2 times higher than that in HLCs without Sch B treatment (Figure 3C). However, there was no significant difference in AFP expression between the groups with and without Sch B treatment (Figures 3B and 3C).

In addition to hepatic markers, liver function was assessed by measuring glycogen storage, albumin secretion, and urea synthesis. Albumin secretion was increased after induction and Sch B-treated HLCs showed higher secretion of albumin as compared with untreated cells (Figure 3D). Similarly, in HLCs, urea production was higher with than without Sch B treatment at the endpoint of the differentiation process

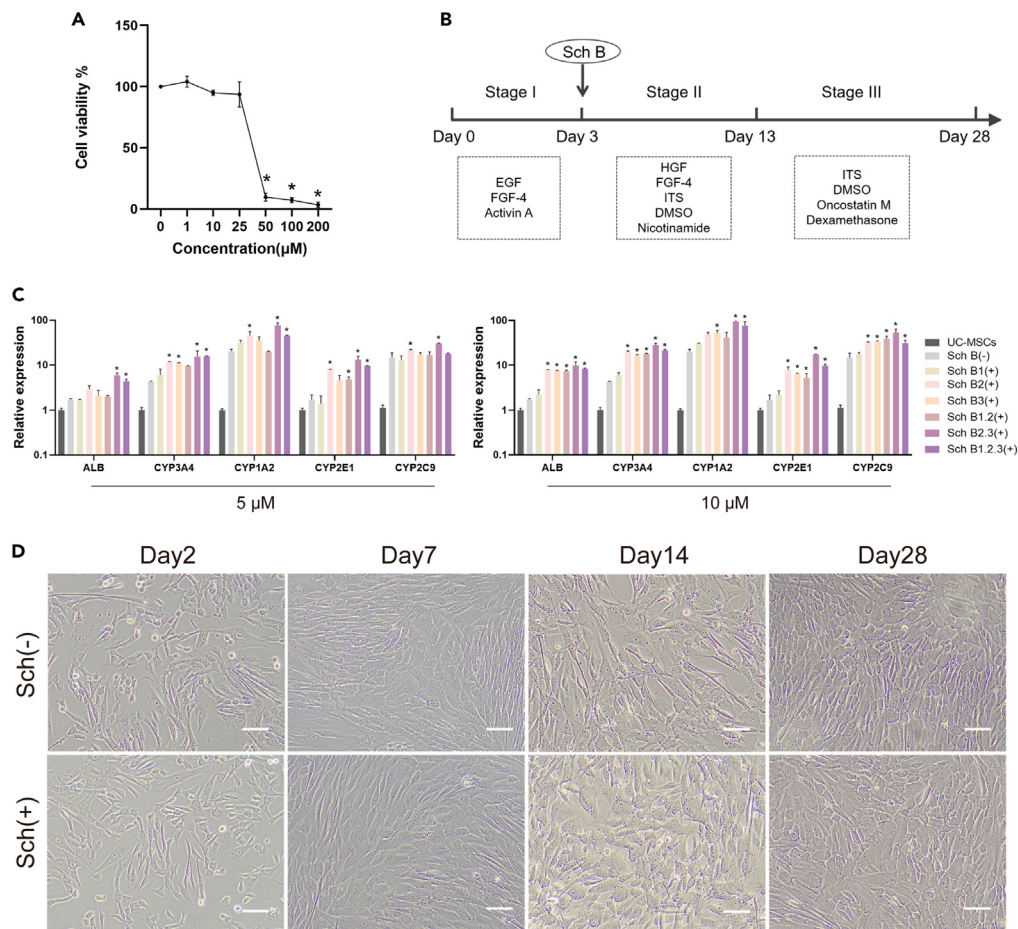


**Figure 2. Determining the optimal concentration and treatment time of Sch B**

(A) UC-MSCs were treated with 0–200 µM Sch B for 72 h. Cell viability was assessed by CCK-8 assay.

(B) Schematic diagram of UC-MSCs differentiated into hepatocytes.

(C) The mRNA levels of hepatic markers (ALB, CYP3A4, CYP1A2, CYP2E1 and CYP2C9) were determined by qPCR analysis in UC-MSCs and cells with Sch B(–) (without Sch B treatment), Sch B1(+) (Sch B treatment only at first stage), Sch B2(+) (Sch B treatment only at second stage), Sch B3(+) (Sch B treatment only at third stage), Sch B1.2(+) (Sch B treatment at first and second stage), Sch B2.3(+) (Sch B treatment at second and third stage), Sch B1.2.3(+) (Sch B treatment at first, second and third stage).

(D) Morphological changes of UC-MSCs differentiated into hepatocytes with or without Sch B treatment. Scale bar = 100 µm. Graph data were presented as mean ± SD. One-way ANOVA was used for multiple variables comparison. \*p < 0.05, \*\*p < 0.01, \*\*\*p < 0.001 versus the Sch B(–) group. EGF: epidermal growth factor; FGF-4: fibroblast growth factor 4; HGF: hepatocyte growth factor; ITS: insulin-transferrin-selenium; DMSO: dimethyl sulfoxide.

(Figure 3E). Periodic acid-Schiff (PAS) staining was negative in undifferentiated UC-MSCs; however, Sch B-treated cells showed more glycogen deposition than untreated cells (Figure 3F).

Furthermore, to verify the long-term stability of HLCs, cells were continuously cultured using the third-stage medium after induction. Following an additional 28 days of cultivation (passaged every 7 days), the cell viability and functionality were assessed. Notably, the cells maintained their morphology and exhibited high cell viability. And the Sch B-treated HLCs continued to express hepatic markers, maintain albumin secretion and glycogen storage function (Figure S2). Therefore, these results strongly demonstrated that Sch B could improve the strategy for differentiation of UC-MSCs into HLCs.

### Transcriptome sequencing analysis

To obtain a global view of transcriptome changes during the hepatic differentiation of UC-MSCs, we used transcriptome sequencing of undifferentiated UC-MSCs with Sch B(–) and Sch B(+) treatment. On average, more 40 million raw reads were obtained from each sample. After quality control, about 92% of reads were clean reads. More than 93% of reads could be mapped to the reference genome.

Comparisons between each treatment group revealed differentially expressed genes (DEGs). We found 314 DEGs between Sch B(–) and Sch B(+) treatment (Figure 4A). A Venn diagram shows the number of DEGs between comparison groups and the overlap (Figure 4B). Several genes

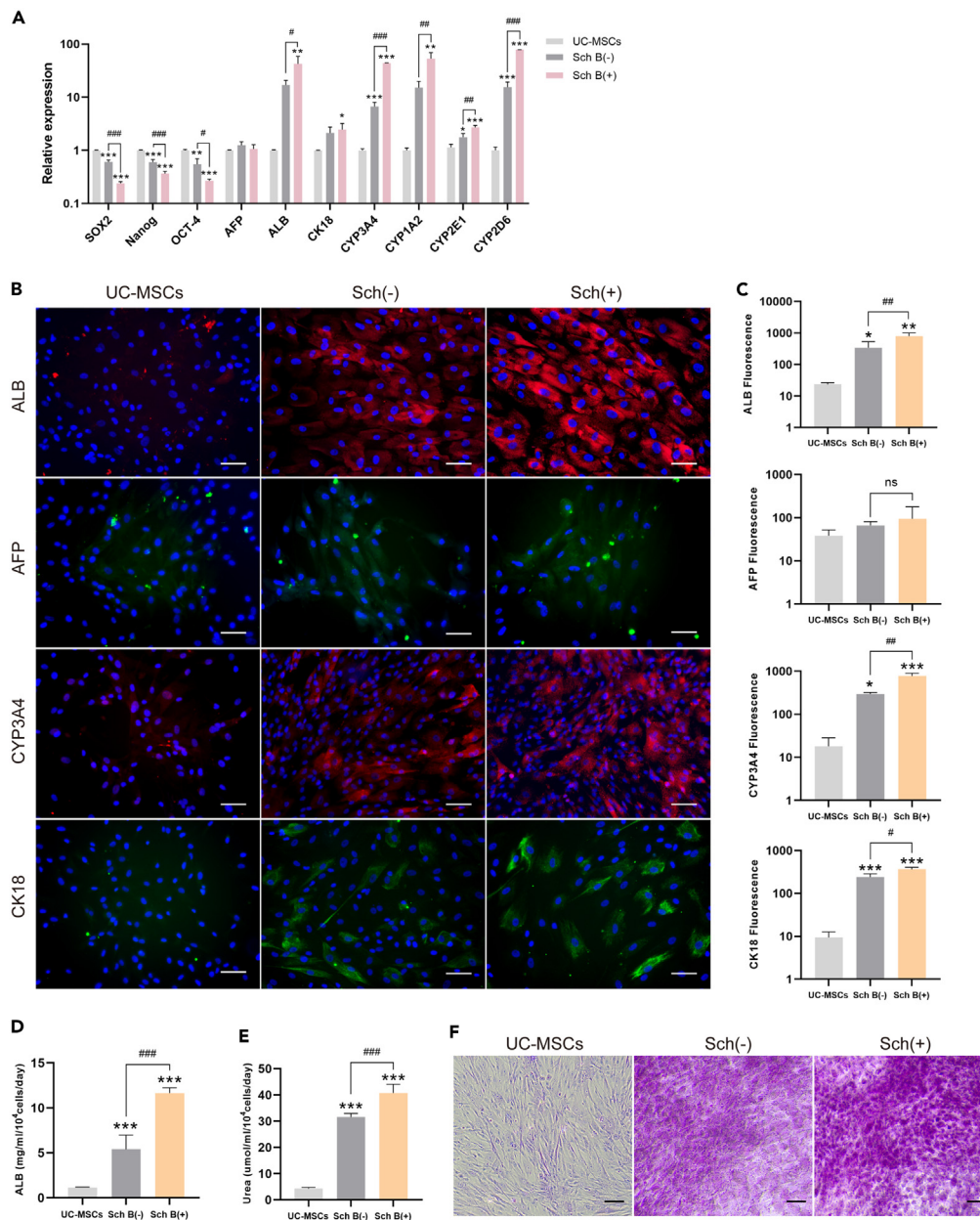


**Figure 3. Enhancement of hepatocyte differentiation and maturation by Sch B**

(A) The mRNA levels of stemness markers and hepatic markers determined by qPCR analysis.

(B and C) Immunofluorescence analysis of ALB, AFP, CK18, and CYP3A4 in UC-MSCs differentiated into hepatocytes with or without Sch B. Scale bar = 50  $\mu$ m.

(D) ELISA of secretion of ALB in differentiated UC-MSCs with or without Sch B.

(E) ELISA of urea production in differentiated UC-MSCs with or without Sch B.

(F) Glycogen storage characterized by PAS staining in differentiated UC-MSCs with or without Sch B. Scale bar = 100  $\mu$ m. Graph data were presented as mean  $\pm$  SD. One-way ANOVA was used for multiple variables comparison. \* $p < 0.05$ , \*\* $p < 0.01$ , \*\*\* $p < 0.001$  versus the UC-MSCs group, # $p < 0.05$ , ## $p < 0.01$ , ### $p < 0.001$  versus the Sch B(-) group. n.s., no significance in comparison with control group. PAS: periodic acid-Schiff.

such as IL6ST, PRLR, PIK3R3, SOCS3, APC, CXCL12, ATM, RIF1, IGFBP3, CD14, FASN and CCN4 played important roles in stem cell differentiation. Cluster analysis was used to determine the expression patterns of DEGs under different processing conditions. Because similar expression patterns of genes usually have a correlation function, hierarchical clustering analysis was performed and the results are shown in Figure 4C.

To reveal the biological process pathways of Sch B acting on the hepatic differentiation of UC-MSCs, we analyzed DEGs by GO and KEGG pathway analyses. GO results were classified according to molecular function (MF), biological process (BP) and cellular component (CC), and

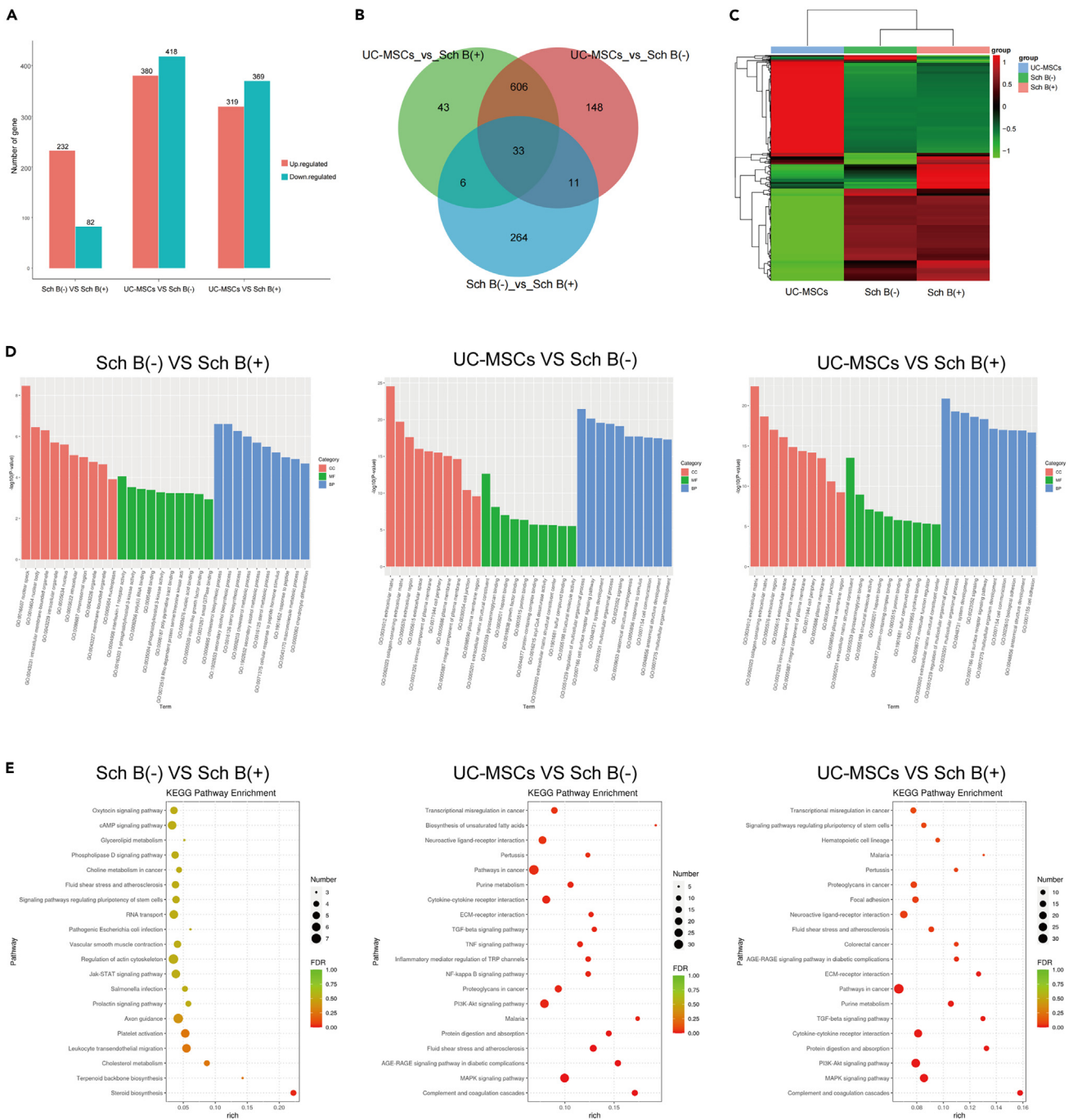


**Figure 4. Transcriptome analysis of differentiated UC-MSCs**

- (A) Number of differentially expressed genes (DEGs) in differentiated UC-MSCs with or without Sch B treatment.  
 (B) Venn diagram of the number of separate and overlapping DEGs between UC-MSCs and HLCs.  
 (C) Cluster analysis (heatmap) of DEGs among UC-MSCs and HLCs.  
 (D) GO analysis of UC-MSCs and HLCs.  
 (E) KEGG analysis of the most significantly enriched pathways for DEGs among UC-MSCs and HLCs.

the top 10 GO terms with most significant enrichment from each GO category are shown in Figure 4D. As compared with undifferentiated UC-MSCs, both HLC treatment groups showed similar main biological functions of the DEGs. After Sch B treatment, CC was mostly related to nuclear speck, nuclear body, chromosomal region, and organelle. In terms of MF, the most enriched terms were interleukin-1 receptor activity,

1-phosphatidylinositol-3-kinase activity, poly(U) RNA binding, phosphatidylinositol 3-kinase activity, insulin-like growth factor binding, and small GTPase binding. In addition, BP items enriched after Sch B treatment included cholesterol biosynthetic and metabolic process, secondary alcohol biosynthetic and metabolic process, macromolecule metabolic process and chondrocyte differentiation.

Next, KEGG pathway enrichment analysis was performed to identify the most significantly enriched pathways for DEGs (Figure 4E). As compared with undifferentiated UC-MSCs, the most enriched pathways with differentiation included the TGF- $\beta$ , NF- $\kappa$ B, PI3K-Akt and MAPK signaling pathways. In addition, the JAK-STAT signaling pathway, regulation of action cytoskeleton, signaling pathways regulating pluripotency of stem cells, oxytocin signaling pathway, platelet activation, and steroid biosynthesis were enriched in DEGs between Sch B(–) and Sch B(+) groups.

### Validation of sequencing results and signaling pathways affected by Sch B

To validate the reliability of the DEG results, qPCR was used to examine the expression of several upregulated genes (PRLR, JAK2, STAT3, RORA, ALB) and downregulated genes (BGN, ILR7, THY1, SPRED3, NR5A2). Primers used in this study are in Table S1. As expected, the qPCR results matched the RNA-seq results (Figure S3).

We found that genes involved in the JAK-STAT signaling pathway were upregulated in Sch B-treated cells. We evaluated STAT3 downstream targets such as c-Myc, cyclinD1 and HIF-1 $\alpha$ , and both c-Myc and HIF-1 $\alpha$  were upregulated, and cyclinD1 was downregulated (Figure 5A). Furthermore, phosphorylation of JAK2 and STAT3 was increased in Sch B-treated cells (Figure 5B). Both c-Myc and HIF-1 $\alpha$  protein levels were increased and cyclinD1 decreased in Sch B treated cells (Figures 5C and 5D). Next, the JAK2/STAT3 signaling pathway was blocked using Stattic and AG490, resulting in decreased expression of hepatic markers (ALB, CK18, HNF4 $\alpha$ ) in both Stattic-treated and AG490-treated groups (Figures 5E–5G). These results indicate that Sch B enhances the JAK2/STAT3 signaling pathway during the hepatic differentiation procession (Figure 6).

### Transplantation of Sch B treated HLCs significantly alleviate CCL<sub>4</sub>-induced mice liver fibrosis

Gelatin methacryloyl (GelMA) hydrogel is commonly utilized as a cell culture scaffold due to its biocompatibility and ultraviolet (UV) light crosslinking properties. To enable cell transplantation, UC-MSCs and HLCs were co-cultured with GelMA hydrogel to form HLCs-GelMA hydrogel complex. The biocompatibility of the GelMA hydrogel was assessed by monitoring cell activity on days 1, 3, and 7. Live/dead staining revealed sustained high levels of cellular activity in the HLCs (Figure 7B).

We next evaluated the therapeutic potential of HLCs transplantation in CCL<sub>4</sub>-induced chronic liver fibrosis. UC-MSCs-GelMA hydrogel or HLCs-GelMA hydrogel were transplanted onto the surface of liver. The liver and serum were harvested after 7 and 14 days of transplantation (Figure 7C). The liver of CCL<sub>4</sub> group showed a nodular surface and firm texture as compared to the control (oil) group. In contrast, the liver of UC-MSCs and HLCs transplanted groups displayed a smooth surface and soft texture. Additionally, GelMA hydrogels were observed attached to the surface of the liver in the transplantation group (Figure 7D). Hematoxylin and eosin (HE) staining revealed significant hepatocyte degeneration, necrosis and inflammatory cell infiltration in the liver tissue of CCL<sub>4</sub> group. However, these pathological changes were significantly improved after cell transplantation (Figure 7E).

Serum AST and ALT levels were measured to assess the extent of hepatic dysfunction. After 7 days of treatment, the transplantation groups exhibited a significant decrease in ALT and AST levels compared to the CCL<sub>4</sub> group. Notably, the Sch B treated HLCs demonstrated superior therapeutic efficacy compared to the other two transplantation groups. After 14 days of treatment, AST and ALT levels were decreased in all groups, but the HLCs transplantation group treated with Sch B exhibited the most significant decrease (Figures 7F and 7G).

Consistently, Masson staining and Sirius red showed that the collagen contents significant increase in CCL<sub>4</sub>-treated mice liver. However, transplantation of UC-MSCs and HLCs significantly reduced the progression of liver fibrosis (Figures 8A and 8B). Furthermore, we quantified the collagen area and found that it was the lowest in the group treated with Sch B (Figures 8C and 8D). To evaluate the functionality of engrafted cells, human ALB in the liver of transplanted mice was quantified by ELISA. The levels of human ALB in the group treated with Sch B were significantly higher than in the other groups (Figure 8E). In addition, HE staining showed that the graft was tightly attached to the liver surface without extensive inflammatory cell infiltration, and angiogenesis was observed at both the 7-day and 14-day time points after transplantation (Figure S4). Angiogenesis was further confirmed by immunohistochemistry (Figure S4). These results indicate that the graft had good biocompatibility. Taken together, Sch B treated HLCs exhibit higher therapeutic potential against liver fibrosis when compared to HLCs without Sch B treatment and undifferentiated UC-MSCs.

## DISCUSSION

In this study, we investigated the effect of Sch B on the hepatic differentiation of UC-MSCs. Treatment with 10  $\mu$ M Sch B from the second stage of the differentiation process increased hepatic marker levels and hepatic function, including albumin and urea secretion and glycogen storage. Thus, Sch B could enhance the hepatic differentiation and maturation of UC-MSCs. And Sch B enhancing the hepatic differentiation of UC-MSCs may involve the JAK2/STAT3 signaling pathway. In addition, Sch B treated HLCs showed significant therapeutic effects on mice with chronic liver fibrosis. This study provides an optimized hepatic differentiation protocol for UC-MSCs based on Sch B, generating better functioning cells for the treatment of liver disease.

The sources of MSCs are abundant. MSCs can be isolated from various somatic tissues such as adipose tissue, bone marrow, amniotic fluid, placenta, and menstrual blood.<sup>29</sup> Karyotype analysis showed that UC-MSCs originating from the fetus showed high proliferative ability among

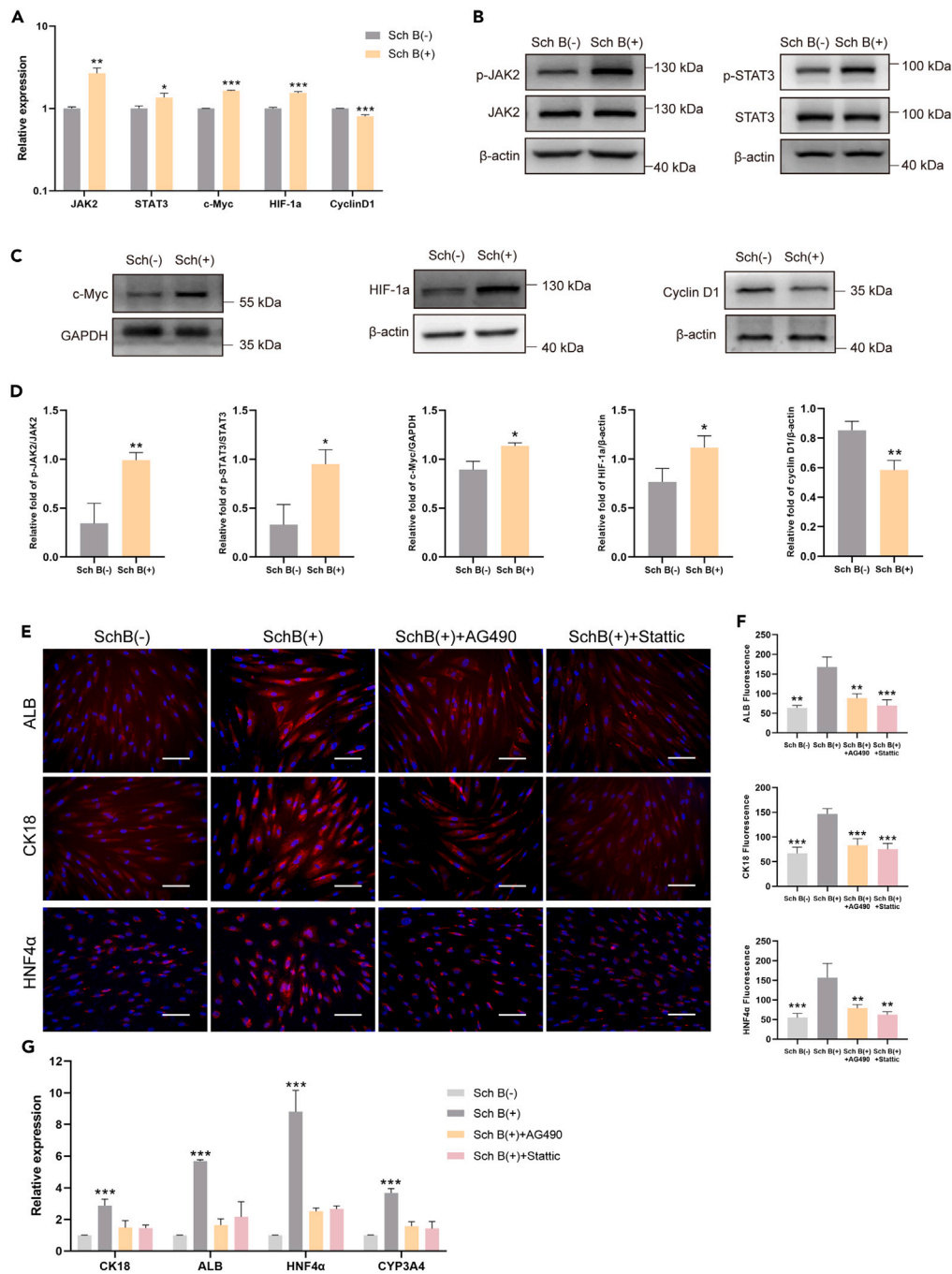


**Figure 5. Validation of signaling pathways affected by Sch B**

(A) qPCR analysis of genes involved in JAK2/STAT3 signaling pathways.

(B) Western blot analysis of the expression of JAK2, phospho-JAK2, STAT3, and phospho-STAT3 in differentiated cells with or without Sch B treatment.

(C) Western blot analysis of the expression of c-Myc, HIF-1α, and cyclinD1 in differentiated cells with or without Sch B treatment.

(D) Quantitative analysis of the protein expression in B and C.

(E and F) Immunofluorescence analysis of ALB, CK18, and HNF4α in UC-MSCs differentiated into hepatocytes with JAK2/STAT3 inhibitor treatment (Stattic and AG490). Scale bar = 50 μm.

(G) mRNA levels of hepatic markers determined by qPCR analysis in UC-MSCs after differentiation into hepatocytes using JAK2/STAT3 inhibitors (Stattic and AG490). Graph data were presented as mean ± SD. Unpaired Student's t tests were used for comparing two variables. One-way ANOVA was used for multiple variables comparison. \*p < 0.05, \*\*p < 0.01, \*\*\*p < 0.001 versus the Sch B(-) group.

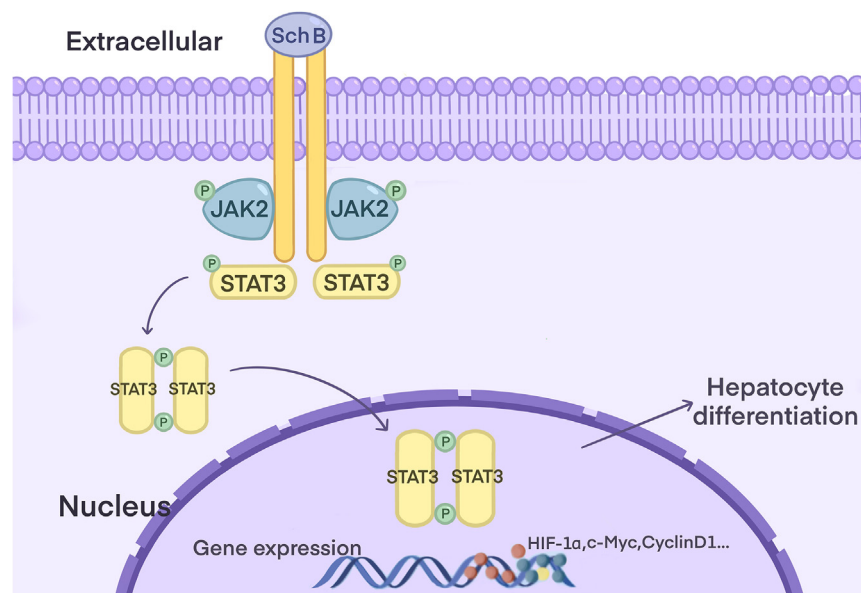


**Figure 6. Illustration of the effects of Sch B on hepatocyte differentiation from UC-MSCs**

several placenta-derived MSCs.<sup>30</sup> In a study comparing the hepatic differentiation ability between UC-MSCs and BM-MSCs, UC-MSC-derived HLCs showed higher expression of ALB, CYP3A4, TAT, and G-6P, so UC-MSCs have higher hepatocyte differentiation potential.<sup>31</sup> In addition, due to fewer ethical concerns, low immunogenicity, and abundant sources, UC-MSCs are an ideal source of cell-based therapies for liver diseases.

The hepatic differentiation of stem cells is basically carried out by mimicking the development of hepatocytes *in vivo*. However, the efficiency of induction varies among laboratories, as do the biological characteristics among different stem cells. In this study, we compared several induction protocols reported in the literature and made some modifications. We finally obtained a serum-free induction protocol according to the characteristics of UC-MSCs. We hope to further optimize the induction protocol to obtain mature HLCs.

In recent years, researchers have focused more on the promotion of small molecule compounds in the targeted differentiation of stem cells, and many effective small molecule compounds have been successfully screened.<sup>32</sup> In contrast, there are few reports of the application of traditional Chinese medicine in stem cell differentiation. Actually, some traditional Chinese medicine has the hepato-protective effect and also promotes the hepatic differentiation of stem cells. Chen et al.<sup>14,15</sup> reported that the Chinese medicine fuzheng huayu and salivianolic acid B could enhance the hepatic differentiation of stem cells via WNT and Notch signaling pathways. *S. chinensis* is a commonly used liver protective drug in clinical practice. Its main component, Sch B, can prevent fibrosis progression, induce CYP enzyme activity and promote liver regeneration.<sup>22</sup> Fuzheng huayu is a combinatorial compound of different Chinese herbs. Most compound preparations pose certain drawbacks, such as instability of active ingredient content, difficulty in quality control due to the variety of ingredients, and challenges in studying disease treatment mechanisms. Additionally, multiple components' metabolism *in vivo* may lead to unpredictable interactions. In contrast, Sch B is a monomer with clear composition, better controllability, and higher safety in applications. However, there has been no previous investigation into the effect of Sch B on the hepatogenic differentiation of stem cells. In this study, we investigated whether Sch B could promote hepatogenic differentiation of stem cells and elucidate the underlying mechanisms involved in this process.

First, we successfully isolated and characterized UC-MSCs. Then CCK-8 assay was used to examine the cytotoxicity of Sch B. Next, various concentrations of Sch B were administered at different stages to assess its impact on the hepatic differentiation of UC-MSCs. The mRNA expression of ALB and several phase I metabolizing enzymes, including CYP3A4, CYP2E1, CYP1A2, and CYP2C9, exhibited an increase, with the highest expression observed when Sch B was initiated from the second stage. These results preliminarily proved that 10  $\mu$ M Sch B has potential to promote the hepatic differentiation of UC-MSCs.

We further verified the effect of the new Sch B differentiation strategy on the differentiation and maturation of UC-MSCs. The mRNA expression of stemness markers OCT-4, Nanog and Sox2 was decreased in Sch B-treated cells, indicating a gradual loss of multipotent capacity in the stem cells.<sup>33</sup> The expression of ALB and CYP3A4, markers of mature hepatocytes, was increased in Sch B-treated cells, and the same trend was observed on immunofluorescence analysis. We then determined the function of HLCs by analyzing glycogen staining and albumin and urea content in supernatant assay. Sch B could enhance the ability of albumin secretion, urea synthesis and glycogen storage of HLCs. With the induction protocol based on Sch B, we successfully obtained more mature and more functional HLCs. At the same time, we observed that Sch B showed a better induction effect compared to the two reported traditional Chinese medicine monomers (Salivianolic acid B and Salidroside).<sup>14,16</sup> Importantly, the HLCs demonstrated the capability of being passaged *in vitro* while maintaining a high level of activity and hepatic function even after 28 days of continued culture. However, scalable production protocols still need to be developed to enhance the differentiated yield and functionality of HLCs derived from UC-MSCs to facilitate clinical application.

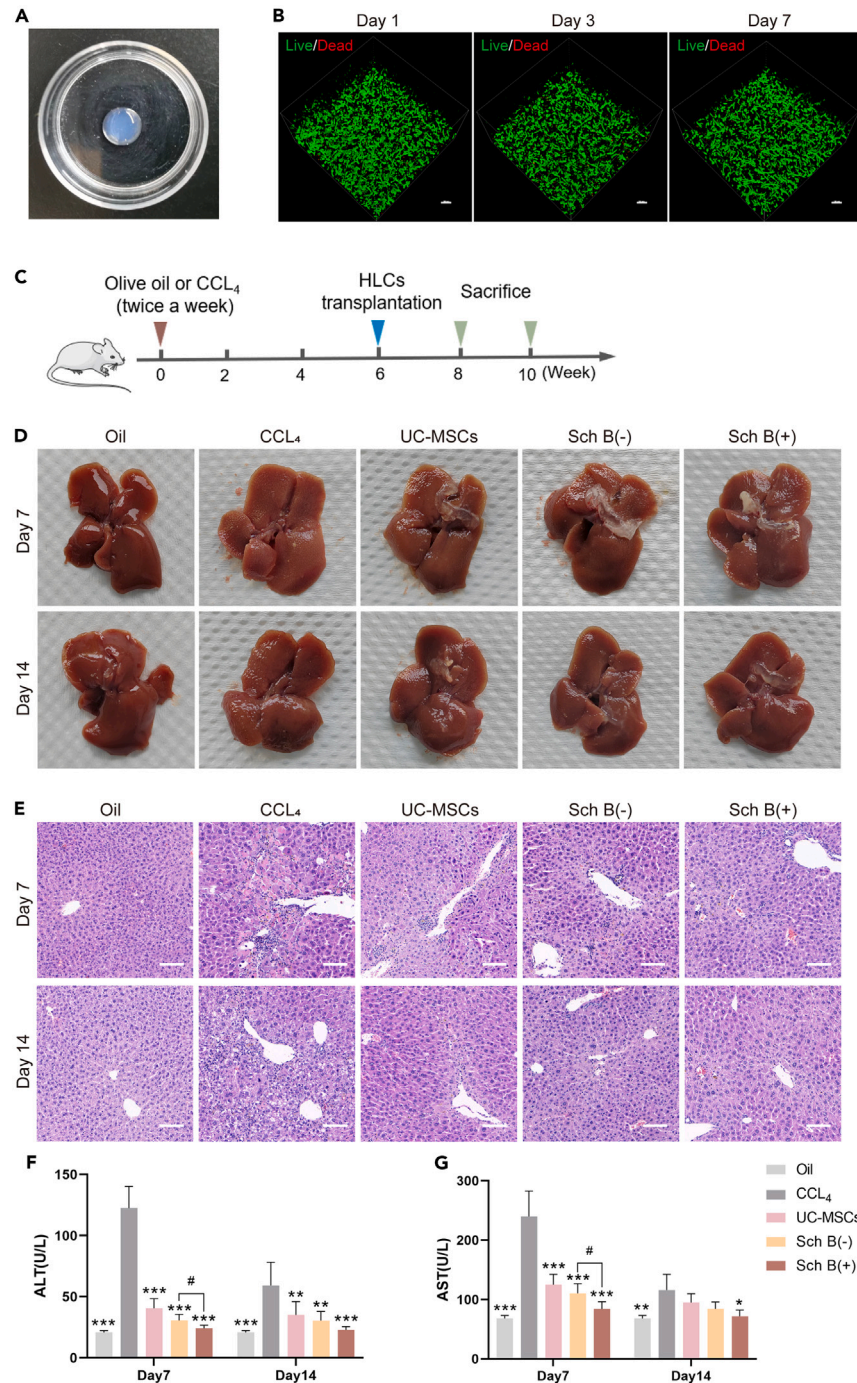


**Figure 7. Sch B treated HLCs transplantation attenuated the CCL<sub>4</sub>-induced chronic liver injury**

(A) Photograph of the HLCs co-cultured with GelMA hydrogel *in vitro*.

(B) Live/Dead staining of HLCs co-culture with GelMA hydrogel at day 1, day 3, and day 7 (Living cells were green and dead cells were red). Scale bar = 100  $\mu$ m.

(C) Schematic diagram of liver fibrosis induction and therapeutic transplantation of HLCs.

(D) Representative images of liver gross appearance after 7 and 14 days' cell transplantation treatment.

(E) HE staining of the liver after 7 and 14 days' cell transplantation treatment. Scale bar = 100  $\mu$ m.

(F and G) Serum levels of ALT and AST after 7 and 14 days' cell transplantation treatment (n = 5). Graph data were presented as mean  $\pm$  SD. One-way ANOVA was used for multiple variables comparison. \*p < 0.05, \*\*p < 0.01, \*\*\*p < 0.001 versus the CCL<sub>4</sub> group, #p < 0.05, ##p < 0.01, ###p < 0.001 versus the Sch B(-) group. Oil: Olive oil group; CCL<sub>4</sub>: CCL<sub>4</sub>-induced liver fibrosis group; UC-MSCs: UC-MSCs transplantation group; Sch B(-): Sch B untreated HLCs transplantation group; Sch B(+): Sch B treated HLCs transplantation group.

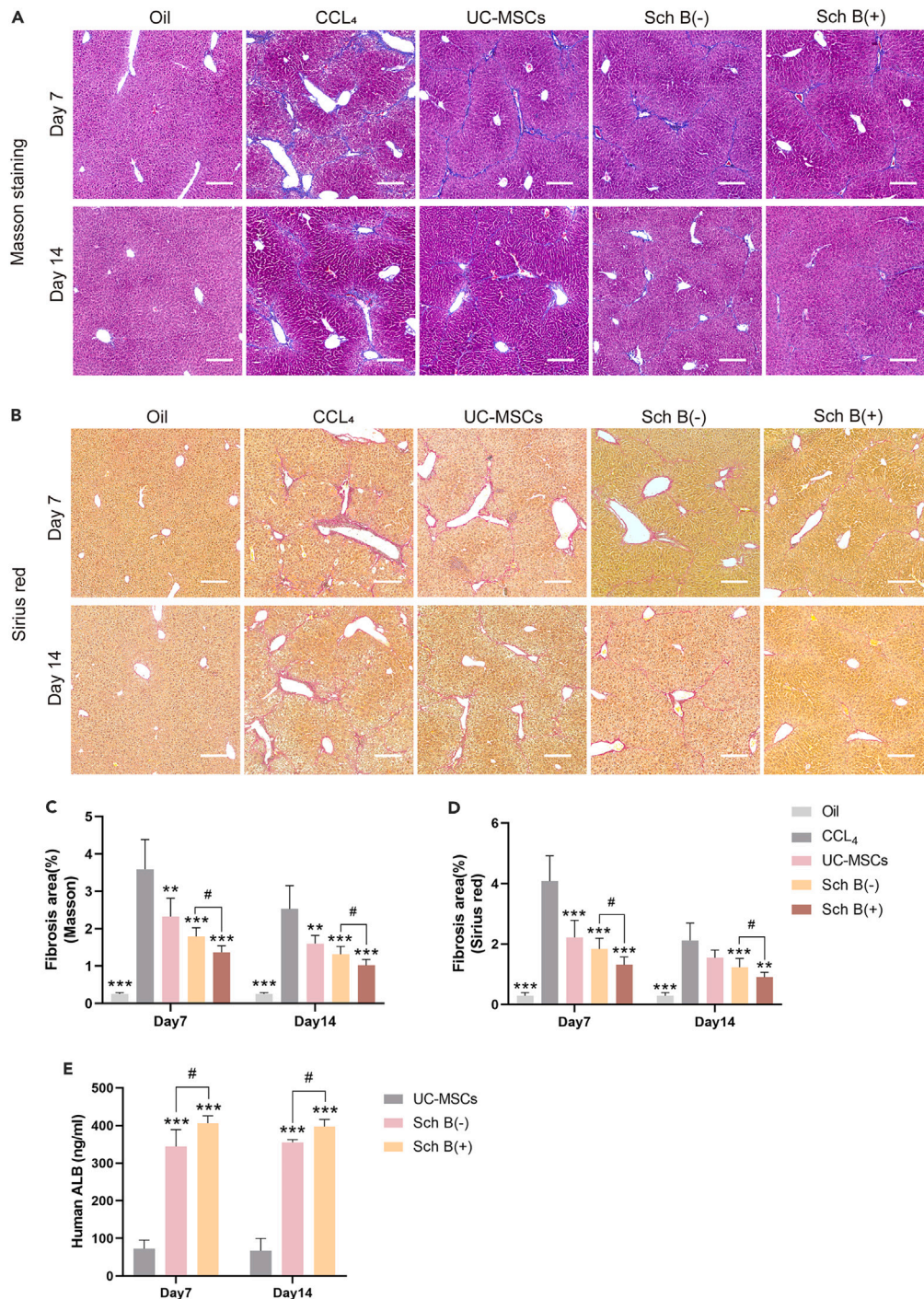


**Figure 8. Sch B treated HLCs transplantation attenuated the CCL<sub>4</sub>-induced mice liver fibrosis**

(A) Representative histological images of liver sections stained with Masson staining. Scale bar = 200  $\mu$ m.

(B) Representative histological images of liver sections stained with Sirius red. Scale bar = 200  $\mu$ m.

(C and D) The Sirius red-positive and Masson staining-positive area was quantified by using ImageJ software. CCL<sub>4</sub> were controls.

(E) At 7 and 14 days after transplantation, human ALB levels of the recipient liver tissues were measured. UC-MSCs were controls. Graph data were presented as mean  $\pm$  SD. One-way ANOVA was used for multiple variables comparison. \* $p < 0.05$ , \*\* $p < 0.01$ , \*\*\* $p < 0.001$  versus the control group, # $p < 0.05$ , ## $p < 0.01$ , ### $p < 0.001$  versus the Sch B(-) group,  $n = 5$ .

Furthermore, RNA-seq revealed the DEGs among those HLCs with Sch B treatment. In the DEGs, we identified several genes most likely to be involved in hepatic differentiation, such as IL6ST, PRLR, PIK3R3, SOCS3, APC, CXCL12, and IGFBP3, which have been reported to be involved in stem cell differentiation.<sup>34–37</sup> *In vivo*, liver development involves a variety of complex pathway mechanisms. Hence, the mechanism of hepatic differentiation of MSCs is also complex. The differentiation of stem cells into hepatocytes is generally divided into three stages, including initiation, differentiation and maturation, and each stage involves different signaling pathways. In general, the signaling pathways involve Wnt/ $\beta$ -catenin, TGF- $\beta$ , Notch, PI3K/AKT, MAPK, and JAK/STAT3 pathways.<sup>38–42</sup> Our KEGG analysis revealed enrichment of PI3K/AKT, TGF- $\beta$ , and MAPK pathways in differentiated versus undifferentiated UC-MSCs. Therefore, our basal induction strategy was effective. Especially, when Sch B was added to the induction process, JAK/STAT3 pathway expression was changed. The JAK/STAT3 pathway is an important signal transduction pathway widely involved in cell proliferation, differentiation, apoptosis, immune regulation, and inflammation.<sup>43</sup> Upon engagement by ligands, receptor-associated JAKs are recruited and activated. Activated JAKs then phosphorylate specific residues on the intracellular domain of the cytokine receptor, which serves as a docking site for associated STAT proteins. JAK-mediated phosphorylation activates STATs, which in turn translocate to the cell nucleus and regulate gene expression.<sup>44</sup> JAK proteins can associate with distinct cytokine receptors, including interferon, interleukin or growth hormone. IL-6R is one of the most common cytokine receptors that bind to JAK proteins. Lam et al.<sup>41</sup> indicated that IL-6-mediated activation of JAK/STAT signaling played a key role in the differentiation of MSCs into hepatocytes. Oncostatin M (OSM), an interleukin-6 family cytokine, is commonly used in the maturation stage of hepatic differentiation.<sup>45</sup> OSM can activate the JAK/STAT3 pathway to induce liver-specific gene expression, mediate hepatocyte differentiation and maturation, and establish cell–cell interactions by regulating HNF-4 expression.<sup>46,47</sup> In addition, Matsui et al.<sup>48</sup> demonstrated that OSM downregulated the expression of cyclin D by activating the STAT3 pathway in primary cultures of fetal hepatocytes induced to hepatic differentiation. Hypoxia is known to play an important role in stem cell differentiation and hepatocyte maturation, and hypoxia is also one of the commonly used induction methods in recent years.<sup>49</sup> Vollmer et al. found that activation of the JAK/STAT3 pathway mediated HIF1a upregulation, which in turn promoted downstream signal transduction events in OSM, thus demonstrating an interaction between cytokines and hypoxia signal transduction during liver development and regeneration.<sup>50</sup>

Our KEGG pathway analysis revealed enriched JAK/STAT pathway signaling. As expected, key genes involved in the JAK/STAT signaling pathway, JAK2 and STAT3, were upregulated, and the expression of target genes, cyclinD1, c-Myc, and HIF1a, which facilitate cell proliferation and differentiation, were altered. In this study, total protein levels of JAK2 and STAT3 were not increased with their mRNA upregulation, but phosphorylated protein levels were increased, which suggests that Sch B may play a role in post-translational modification. Also, blocking JAK2/STAT3 signaling with two commonly used inhibitors (Stattic and AG490) downregulated the expression of hepatic markers. These results suggest that Sch B may activate the JAK2/STAT3 signaling pathway to regulate differentiation and maturation of HLCs.

Next, we evaluated the therapeutic effect of HLCs on mice with chronic liver fibrosis. GelMA hydrogel is widely used in tissue engineering due to its good biocompatibility and excellent mechanical properties.<sup>51</sup> *In vitro*, we observed that HLCs maintained high viability after being cultured in GelMA hydrogel for 7 days. *In vivo*, the cell-GelMA solution rapidly crosslinks within seconds upon UV irradiation, forming a hydrogel patch. Angiogenesis was observed in the patch and no significant infiltration of inflammatory cells was detected, indicating good biocompatibility of the hydrogel patch. Human albumin expression was detected in the liver tissues, indicating that the transplanted cells still maintained hepatic function *in vivo*. The hydrogel not only provides a cellular scaffold, avoiding cell loss, but also acts as a physical barrier against the recipient's immune system.<sup>52</sup> Therefore, we offered a safe and effective transplant treatment strategy. Importantly, after the patch grafting, the levels of ALT and AST significantly decreased. Although undifferentiated UC-MSCs also showed a certain therapeutic effect, it was not as good as observed in the HLCs group. The deposition of liver collagen was significantly reduced in the Sch B group, indicating that HLCs treated with Sch B have the potential to alleviate liver fibrosis and are suitable for treating chronic liver diseases.

Overall, our results suggest that Sch B is able to promote hepatic differentiation from UC-MSCs via activating the JAK2/STAT3 signaling pathway. And we observed that Sch B-treated HLCs significantly decreased collagen deposition and improved liver function in mice with liver fibrosis. Our study provides an optimized hepatic differentiation strategy for UC-MSCs, which will be helpful for generating functional HLCs for future clinical application.

### Limitations of the study

In this study, we first verified that Sch B could promote the differentiation and maturation of UC-MSCs into hepatocytes. Then we confirmed that JAK2/STAT3 pathway activation was involved in this effect of Sch B. Finally, we conducted *in vivo* experiment to assess the potential therapeutic effect of the Sch B treated HLCs on liver fibrosis. Further clinical trials are needed to determine the safety, efficacy, and therapeutic potential of UC-MSCs-derived HLCs in patients with liver disease. However, this study has two limitations. First, we did not compare the function of HLCs induced by our method with that of primary hepatocytes. Second, the mechanism of HLCs alleviating liver fibrosis has not been further investigated.

### STAR★METHODS

Detailed methods are provided in the online version of this paper and include the following:

- [KEY RESOURCES TABLE](#)
- [RESOURCE AVAILABILITY](#)
  - Lead contact
  - Materials availability

- Data and code availability
- **EXPERIMENTAL MODEL AND STUDY PARTICIPANT DETAILS**
  - Cell culture
  - Animal experiments
- **METHOD DETAILS**
  - Isolation and identification of UC-MSCs
  - Hepatocyte differentiation from UC-MSCs
  - Treatment of differentiated cells with Sch B
  - Quantitative real-time PCR analysis
  - Immunofluorescence staining
  - Albumin assay
  - Urea production
  - Periodic acid–Schiff staining
  - Transcriptome sequencing
  - Gene ontology (GO) and KEGG enrichment analysis
  - Western blot analysis
  - Preparation of GelMA hydrogel and biocompatibility assay
  - Establishment and treatment of chronic liver fibrosis model
  - Biochemical assay and histological analysis
- **QUANTIFICATION AND STATISTICAL ANALYSIS**

## SUPPLEMENTAL INFORMATION

Supplemental information can be found online at <https://doi.org/10.1016/j.isci.2024.108912>.

## ACKNOWLEDGMENTS

This work was funded by the Natural Science Foundation of Xinjiang Uygur Autonomous Region (2021D01C011), the President Foundation of Zhujiang Hospital, Southern Medical University (yzjj2022ms13), the National Key R&D Program of China (2018YFA0108200), the Guangdong Basic and Applied Basic Research Foundation (2023A1515012452, 2021B1515230011) and the National Natural Science Foundation of China (81760664, 82072627).

## AUTHOR CONTRIBUTIONS

M.J. was responsible for conceptualization, methodology, validation, and roles/writing-original draft. X.Y. was responsible for methodology. X.Z., Y.L., and S.L. were responsible for resources. Q.C., S.W., W.H., and W.Y. were responsible for validation. Q.P. was responsible for methodology, roles/writing–review and editing, and funding acquisition. M.P. and Y.G. were responsible for funding acquisition. S.X. was responsible for conceptualization, and supervision. Y.Z. was responsible for methodology, formal analysis, data curation. S.Z. was responsible for conceptualization, roles/writing–review and editing, supervision, and funding acquisition. All authors have read and agreed to the published version of the manuscript.

## DECLARATION OF INTERESTS

The authors declare no competing interests.

Received: June 6, 2023

Revised: October 30, 2023

Accepted: January 11, 2024

Published: January 15, 2024

## REFERENCES

1. Luce, E., Messina, A., Duclos-Vallée, J.C., and Dubart-Kupperschmitt, A. (2021). Advanced Techniques and Awaited Clinical Applications for Human Pluripotent Stem Cell Differentiation into Hepatocytes. *Hepatology* 74, 1101–1116.
2. Asrani, S.K., Devarbhavi, H., Eaton, J., and Kamath, P.S. (2019). Burden of liver diseases in the world. *J. Hepatol.* 70, 151–171.
3. Tuerxun, K., He, J., Ibrahim, I., Yusupu, Z., Yasheng, A., Xu, Q., Tang, R., Aikebaier, A., Wu, Y., Tuerdi, M., et al. (2022). Bioartificial livers: a review of their design and manufacture. *Biofabrication* 14, 032003.
4. Lee, C.A., Sinha, S., Fitzpatrick, E., and Dhawan, A. (2018). Hepatocyte transplantation and advancements in alternative cell sources for liver-based regenerative medicine. *J. Mol. Med.* 96, 469–481.
5. Lee, C.W., Chen, Y.F., Wu, H.H., and Lee, O.K. (2018). Historical Perspectives and Advances in Mesenchymal Stem Cell Research for the Treatment of Liver Diseases. *Gastroenterology* 154, 46–56.
6. Berardis, S., Dwisthi Sattwika, P., Najimi, M., and Sokal, E.M. (2015). Use of mesenchymal stem cells to treat liver fibrosis: Current

- situation and future prospects. *World J. Gastroenterol.* 21, 742–758.
7. Chen, Y., Yu, Q., Hu, Y., and Shi, Y. (2019). Current Research and Use of Mesenchymal Stem Cells in the Therapy of Autoimmune Diseases. *Curr. Stem Cell Res. Ther.* 14, 579–582.
  8. Shaikh, M.S., Shahzad, Z., Tash, E.A., Janjua, O.S., Khan, M.I., and Zafar, M.S. (2022). Human Umbilical Cord Mesenchymal Stem Cells: Current Literature and Role in Periodontal Regeneration. *Cells* 11.
  9. Fan, X.L., Zhang, Y., Li, X., and Fu, Q.L. (2020). Mechanisms underlying the protective effects of mesenchymal stem cell-based therapy. *Cell. Mol. Life Sci.* 77, 2771–2794.
  10. Yang, X., Meng, Y., Han, Z., Ye, F., Wei, L., and Zong, C. (2020). Mesenchymal stem cell therapy for liver disease: full of chances and challenges. *Cell Biosci.* 10, 123.
  11. Snykers, S., De Kock, J., Rogiers, V., and Vanhaecke, T. (2009). In Vitro Differentiation of Embryonic and Adult Stem Cells into Hepatocytes: State of the Art. *Stem Cell.* 27, 577–605.
  12. Kvist, A.J., Kanebratt, K.P., Walentinsson, A., Palmgren, H., O'Hara, M., Björkbom, A., Andersson, L.C., Ahlqvist, M., and Andersson, T.B. (2018). Critical differences in drug metabolic properties of human hepatic cellular models, including primary human hepatocytes, stem cell derived hepatocytes, and hepatoma cell lines. *Biochem. Pharmacol.* 155, 124–140.
  13. Baxter, M., Withey, S., Harrison, S., Segeritz, C.P., Zhang, F., Atkinson-Dell, R., Rowe, C., Gerrard, D.T., Sison-Young, R., Jenkins, R., et al. (2015). Phenotypic and functional analyses show stem cell-derived hepatocyte-like cells better mimic fetal rather than adult hepatocytes. *J. Hepatol.* 62, 581–589.
  14. Chen, J., Tschudy-Seney, B., Ma, X., Zern, M.A., Liu, P., and Duan, Y. (2018). Salvianolic Acid B Enhances Hepatic Differentiation of Human Embryonic Stem Cells Through Upregulation of WNT Pathway and Inhibition of Notch Pathway. *Stem Cell. Dev.* 27, 252–261.
  15. Chen, J., Gao, W., Zhou, P., Ma, X., Tschudy-Seney, B., Liu, C., Zern, M.A., Liu, P., and Duan, Y. (2016). Enhancement of hepatocyte differentiation from human embryonic stem cells by Chinese medicine Fuzhenghuayu. *Sci. Rep.* 6, 18841.
  16. Ouyang, J.F., Lou, J., Yan, C., Ren, Z.H., Qiao, H.X., and Hong, D.S. (2010). In-vitro promoted differentiation of mesenchymal stem cells towards hepatocytes induced by salidroside. *J. Pharm. Pharmacol.* 62, 530–538.
  17. Li, X., Yang, H., Xiao, J., Zhang, J., Zhang, J., Liu, M., Zheng, Y., and Ma, L. (2020). Network pharmacology based investigation into the bioactive compounds and molecular mechanisms of Schisandrae Chinensis Fructus against drug-induced liver injury. *Bioorg. Chem.* 96, 103553.
  18. Zeng, X., Li, X., Xu, C., Jiang, F., Mo, Y., Fan, X., Li, Y., Jiang, Y., Li, D., Huang, M., and Bi, H. (2017). Schisandra sphenanthera extract (Wuzhi Tablet) protects against chronic-binge and acute alcohol-induced liver injury by regulating the NRF2-ARE pathway in mice. *Acta Pharm. Sin.* B 7, 583–592.
  19. Li, X., Fan, X., Li, D., Zeng, X., Zeng, H., Wang, Y., Zhou, Y., Chen, Y., Huang, M., and Bi, H. (2016). Schisandra sphenanthera Extract Facilitates Liver Regeneration after Partial Hepatectomy in Mice. *Drug Metab. Dispos.* 44, 647–652.
  20. Nasser, M.I., Zhu, S., Chen, C., Zhao, M., Huang, H., and Zhu, P. (2020). A Comprehensive Review on Schisandrin B and Its Biological Properties. *Oxid. Med. Cell. Longev.* 2020, 2172740.
  21. Hu, Y., Li, H., Li, R., Tian, Y., and Wu, Z. (2021). Protective effects of Schisandrin B against D-GalN-induced cell apoptosis in human hepatocyte (L02) cells via modulating Bcl-2 and Bax. *Bioengineered* 12, 7205–7214.
  22. Zhang, H., Chen, Q., Dahan, A., Xue, J., Wei, L., Tan, W., and Zhang, G. (2019). Transcriptomic analyses reveal the molecular mechanisms of schisandrin B alleviates CCl4-induced liver fibrosis in rats by RNA-sequencing. *Chem. Biol. Interact.* 309, 108675.
  23. Fan, S., Liu, C., Jiang, Y., Gao, Y., Chen, Y., Fu, K., Yao, X., Huang, M., and Bi, H. (2019). Lignans from Schisandra sphenanthera protect against lithocholic acid-induced cholestasis by pregnane X receptor activation in mice. *J. Ethnopharmacol.* 245, 112103.
  24. Zhang, W., Sun, Z., and Meng, F. (2017). Schisandrin B Ameliorates Myocardial Ischemia/Reperfusion Injury Through Attenuation of Endoplasmic Reticulum Stress-Induced Apoptosis. *Inflammation* 40, 1903–1911.
  25. Shi, H., Yan, Y., Yang, H., Pu, P., and Tang, H. (2022). Schisandrin B Diet Inhibits Oxidative Stress to Reduce Ferroptosis and Lipid Peroxidation to Prevent Pirarubicin-Induced Hepatotoxicity. *BioMed Res. Int.* 2022, 5623555.
  26. Lai, Q., Luo, Z., Wu, C., Lai, S., Wei, H., Li, T., Wang, Q., and Yu, Y. (2017). Attenuation of cyclosporine A induced nephrotoxicity by schisandrin B through suppression of oxidative stress, apoptosis and autophagy. *Int. Immunopharm.* 52, 15–23.
  27. Cai, N.N., Geng, Q., Jiang, Y., Zhu, W.Q., Yang, R., Zhang, B.Y., Xiao, Y.F., Tang, B., and Zhang, X.M. (2022). Schisandrin A and B affect the proliferation and differentiation of neural stem cells. *J. Chem. Neuroanat.* 119, 102058.
  28. Dominici, M., Le Blanc, K., Mueller, I., Slaper-Cortenbach, I., Marini, F., Krause, D., Deans, R., Keating, A., Prockop, D., and Horwitz, E. (2006). Minimal criteria for defining multipotent mesenchymal stromal cells. The International Society for Cellular Therapy position statement. *Cytotherapy* 8, 315–317.
  29. Jin, M., Yi, X., Liao, W., Chen, Q., Yang, W., Li, Y., Li, S., Gao, Y., Peng, Q., and Zhou, S. (2021). Advancements in stem cell-derived hepatocyte-like cell models for hepatotoxicity testing. *Stem Cell Res. Ther.* 12, 84.
  30. Yi, X., Chen, F., Liu, F., Peng, Q., Li, Y., Li, S., Du, J., Gao, Y., and Wang, Y. (2020). Comparative separation methods and biological characteristics of human placental and umbilical cord mesenchymal stem cells in serum-free culture conditions. *Stem Cell Res. Ther.* 11, 183.
  31. Yu, Y.B., Song, Y., Chen, Y., Zhang, F., and Qi, F.Z. (2018). Differentiation of umbilical cord mesenchymal stem cells into hepatocytes in comparison with bone marrow mesenchymal stem cells. *Mol. Med. Rep.* 18, 2009–2016.
  32. Du, C., Feng, Y., Qiu, D., Xu, Y., Pang, M., Cai, N., Xiang, A.P., and Zhang, Q. (2018). Highly efficient and expedited hepatic differentiation from human pluripotent stem cells by pure small-molecule cocktails. *Stem Cell Res. Ther.* 9, 58.
  33. Lau, T.T., Ho, L.W., and Wang, D.A. (2013). Hepatogenesis of murine induced pluripotent stem cells in 3D micro-cavitary hydrogel system for liver regeneration. *Biomaterials* 34, 6659–6669.
  34. Ogueta, S., Muñoz, J., Obregon, E., Delgado-Baeza, E., and García-Ruiz, J.P. (2002). Prolactin is a component of the human synovial liquid and modulates the growth and chondrogenic differentiation of bone marrow-derived mesenchymal stem cells. *Mol. Cell. Endocrinol.* 190, 51–63.
  35. Wei, H., Wang, J., Xu, Z., Li, W., Wu, X., Zhuo, C., Lu, Y., Long, X., Tang, Q., and Pu, J. (2021). Hepatoma Cell-Derived Extracellular Vesicles Promote Liver Cancer Metastasis by Inducing the Differentiation of Bone Marrow Stem Cells Through microRNA-181d-5p and the FAK/Src Pathway. *Front. Cell Dev. Biol.* 9, 607001.
  36. Liu, H., Yi, X., Tu, S., Cheng, C., and Luo, J. (2021). Kaempferol promotes BMSC osteogenic differentiation and improves osteoporosis by downregulating miR-10a-3p and upregulating CXCL12. *Mol. Cell. Endocrinol.* 520, 111074.
  37. Kim, J.H., Yoon, S.M., Song, S.U., Park, S.G., Kim, W.S., Park, I.G., Lee, J., and Sung, J.H. (2016). Hypoxia Suppresses Spontaneous Mineralization and Osteogenic Differentiation of Mesenchymal Stem Cells via IGFBP3 Up-Regulation. *Int. J. Mol. Sci.* 17, 1389.
  38. Li, Z., Wu, J., Wang, L., Han, W., Yu, J., Liu, X., Wang, Y., Zhang, Y., Feng, G., Li, W., et al. (2019). Generation of qualified clinical-grade functional hepatocytes from human embryonic stem cells in chemically defined conditions. *Cell Death Dis.* 10, 763.
  39. Touboul, T., Chen, S., To, C.C., Mora-Castilla, S., Sabatini, K., Tukey, R.H., and Laurent, L.C. (2016). Stage-specific regulation of the WNT/beta-catenin pathway enhances differentiation of hESCs into hepatocytes. *J. Hepatol.* 64, 1315–1326.
  40. Magner, N.L., Jung, Y., Wu, J., Nolte, J.A., Zern, M.A., and Zhou, P. (2013). Insulin and igfs enhance hepatocyte differentiation from human embryonic stem cells via the PI3K/AKT pathway. *Stem Cell.* 31, 2095–2103.
  41. Lam, S.P., Luk, J.M., Man, K., Ng, K.T.P., Cheung, C.K., Rose-John, S., and Lo, C.M. (2010). Activation of interleukin-6-induced glycoprotein 130/signal transducer and activator of transcription 3 pathway in mesenchymal stem cells enhances hepatic differentiation, proliferation, and liver regeneration. *Liver Transplant.* 16, 1195–1206.
  42. Ye, J.S., Su, X.S., Stoltz, J.F., de Isla, N., and Zhang, L. (2015). Signalling pathways involved in the process of mesenchymal stem cells differentiating into hepatocytes. *Cell Prolif.* 48, 157–165.
  43. Xin, P., Xu, X., Deng, C., Liu, S., Wang, Y., Zhou, X., Ma, H., Wei, D., and Sun, S. (2020). The role of JAK/STAT signaling pathway and its inhibitors in diseases. *Int. Immunopharm.* 80, 106210.
  44. O'Shea, J.J., Schwartz, D.M., Villarino, A.V., Gadina, M., McInnes, I.B., and Laurence, A. (2015). The JAK-STAT pathway: impact on human disease and therapeutic intervention. *Annu. Rev. Med.* 66, 311–328.
  45. Natale, A., Vanmol, K., Arslan, A., Van Vlierberghe, S., Dubrue, P., Van Erps, J., Thienpont, H., Buzgo, M., Boeckmans, J., De Kock, J., et al. (2019). Technological advancements for the development of stem

- cell-based models for hepatotoxicity testing. *Arch. Toxicol.* 93, 1789–1805.
46. Ito, Y., Matsui, T., Kamiya, A., Kinoshita, T., and Miyajima, A. (2000). Retroviral gene transfer of signaling molecules into murine fetal hepatocytes defines distinct roles for the STAT3 and ras pathways during hepatic development. *Hepatology* 32, 1370–1376.
  47. Kamiya, A., Kinoshita, T., and Miyajima, A. (2001). Oncostatin M and hepatocyte growth factor induce hepatic maturation via distinct signaling pathways. *FEBS Lett.* 492, 90–94.
  48. Matsui, T., Kinoshita, T., Hirano, T., Yokota, T., and Miyajima, A. (2002). STAT3 Down-regulates the Expression of Cyclin D during Liver Development. *J. Biol. Chem.* 277, 36167–36173.
  49. Samal, J.R.K., Rangasami, V.K., Samanta, S., Varghese, O.P., and Oommen, O.P. (2021). Discrepancies on the Role of Oxygen Gradient and Culture Condition on Mesenchymal Stem Cell Fate. *Adv. Healthcare Mater.* 10, e2002058.
  50. Vollmer, S., Kappler, V., Kaczor, J., Flügel, D., Rolvering, C., Kato, N., Kietzmann, T., Behrmann, I., and Haan, C. (2009). Hypoxia-inducible factor 1 $\alpha$  is up-regulated by oncostatin M and participates in oncostatin M signaling. *Hepatology* 50, 253–260.
  51. Li, S., Sun, J., Yang, J., Yang, Y., Ding, H., Yu, B., Ma, K., and Chen, M. (2023). Gelatin methacryloyl (GelMA) loaded with concentrated hypoxic pretreated adipose-derived mesenchymal stem cells(ADSCs) conditioned medium promotes wound healing and vascular regeneration in aged skin. *Biomater. Res.* 27, 11.
  52. Zhang, W., Lanzoni, G., Hani, H., Overi, D., Cardinale, V., Simpson, S., Pitman, W., Allen, A., Yi, X., Wang, X., et al. (2021). Patch grafting, strategies for transplantation of organoids into solid organs such as liver. *Biomaterials* 277, 121067.
  53. Campard, D., Lysy, P.A., Najimi, M., and Sokal, E.M. (2008). Native Umbilical Cord Matrix Stem Cells Express Hepatic Markers and Differentiate Into Hepatocyte-like Cells. *Gastroenterology* 134, 833–848.

## STAR★METHODS

### KEY RESOURCES TABLE

REAGENT or RESOURCE	SOURCE	IDENTIFIER
<b>Antibodies</b>		
PE Mouse anti-Human CD105	BD Sciences	Cat#560839; RRID: AB_2033932
PE Mouse Anti-Human CD90	BD Sciences	Cat#561970; RRID: AB_395970
APC Mouse anti-Human CD73	BD Sciences	Cat#560847; RRID: AB_10612019
APC Mouse Anti-Human CD14	BD Sciences	Cat#561708; RRID: AB_398596
PE Mouse Anti-Human CD34	BD Sciences	Cat#560941; RRID: AB_396151
PE Mouse Anti-Human HLA-DR	BD Sciences	Cat#560943; RRID: AB_396146
Rabbit monoclonal anti-AFP	Abcam	Cat#ab169552; RRID: AB_2756827
Mouse monoclonal anti-CK18	Abcam	Cat#ab668; RRID: AB_305647
Mouse monoclonal anti-CYP3A4	GeneTex	Cat#GTX60577; RRID: AB_2887981
Rabbit monoclonal anti-ALB	Abcam	Cat#ab207327; RRID: AB_2755031
Rabbit monoclonal anti-HNF4 $\alpha$	Abcam	Cat#ab92378; RRID: AB_10562973
Rabbit monoclonal anti-JAK2	Cell Signaling Technology	Cat#3230; RRID: AB_2128522
Rabbit monoclonal anti-phospho-JAK2 (Y1007 + Y1008)	Abcam	Cat#ab32101; RRID: AB_775808
Rabbit monoclonal anti-STAT3	Cell Signaling Technology	Cat#4904; RRID: AB_331269
Rabbit monoclonal anti-phospho-STAT3 (Y705)	Abcam	Cat#ab76315; RRID: AB_1658549
Mouse monoclonal anti-HIF-1 $\alpha$	Santa Cruz Biotechnology	Cat#sc-13515; RRID: AB_627723
Mouse monoclonal anti-Cyclin D1	Proteintech	Cat#60186-1-Ig; RRID: AB_10793718
Rabbit monoclonal anti-c-Myc	Abmart	Cat#T55150; RRID: AB_2934184
Rabbit polyclonal anti-beta actin	Affinity	Cat#AF7018; RRID: AB_2839420
Rabbit polyclonal anti-GAPDH	Affinity	Cat#AF7021; RRID: AB_2839421
Mouse monoclonal anti-CD31	Cell Signaling Technology	Cat#3528; RRID: AB_2160882
<b>Biological samples</b>		
Human umbilical cord samples	Zhujiang Hospital of Southern Medical University	N/A
<b>Chemicals, peptides, and recombinant proteins</b>		
Recombinant human EGF	Peptotech	Cat#AF-100-15
Recombinant Human/Mouse/Rat Activin A	Novoprotein	Cat#C687
Recombinant Human FGF-4	Peptotech	Cat#AF-100-31
Recombinant human HGF	Peptotech	Cat#100-39
Nicotinamide	Sigma	Cat#N0636
Dimethyl sulfoxide	MP Biomedicals	Cat#196055
Insulin-transferrin-selenium	Gibco	Cat#41400045
Oncostatin M	Peptotech	Cat#300-10
Dexamethasone	Sigma	Cat#D4902
Schisandrin B	MedChemExpress	Cat#HY-N0089
Salidroside	MedChemExpress	Cat#HY-N0109
Salvianolic acid B	MedChemExpress	Cat#HY-N1362
<b>Critical commercial assays</b>		
MesenCult™ Adipogenic Differentiation Kit (Human)	Stem cell Technologies	Cat#05412
MesenCult™ Osteogenic Differentiation Kit (Human)	Stem cell Technologies	Cat#05465
Mesenchymal Stem Cell Neurogenic Differentiation Medium	Promocell	Cat#C-28015

(Continued on next page)

**Continued**

REAGENT or RESOURCE	SOURCE	IDENTIFIER
Cell Counting Kit-8	ApexBio Technology	Cat#K1018
M-MLV reverse transcriptase	Accurate Biology	Cat#AG11711
SYBR Green Premix Pro Taq HS qPCR Kit	Accurate Biology	Cat#AG11701
Human albumin ELISA kit	Mlbio	Cat#ml059979
Human urea ELISA kit	Mlbio	Cat#ml643105
Periodic acid–Schiff (PAS)	Solarbio	Cat#G1280
Sirius Red Stain kit	Solarbio	Cat#G1472
Masson trichrome staining kit	ZSGB-BIO	Cat#BSBA-4079B
DAB kit	ZSGB-BIO	Cat#ZLI-9018
Live/Dead Assay Kit	KeyGEN BioTECH	Cat#KGAF001
<b>Deposited data</b>		
Raw data of RNA-seq	This paper	SRA: PRJNA1050632
<b>Experimental models: Organisms/strains</b>		
Mouse: C57BL/6J male mice (6–8 weeks)	Guangdong Slack Jingda Experimental Animal Co., Ltd.	N/A
<b>Oligonucleotides</b>		
Primers see <a href="#">Table S1</a>	This paper	N/A
<b>Software and algorithms</b>		
GraphPad Prism	GraphPad	<a href="https://www.graphpad.com/scientificsoftware/prism/">https://www.graphpad.com/scientificsoftware/prism/</a>
Image J	NIH	<a href="https://imagej.nih.gov/ij/">https://imagej.nih.gov/ij/</a>
<b>Other</b>		
AM-V Serum Free Medium	TBDscience	Cat#sc-82013-G
Penicillin and streptomycin	Gibco	Cat#10378016

**RESOURCE AVAILABILITY****Lead contact**

Further information and requests for resources and reagents should be directed to and will be fulfilled by the lead contact, Shuqin Zhou ([zhoushuqin@smu.edu.cn](mailto:zhoushuqin@smu.edu.cn)).

**Materials availability**

All materials used in this study are either commercially available or through collaboration, as indicated.

**Data and code availability**

- RNA-seq data are publically available at SRA database ([key resources table](#), SRA: PRJNA1050632). All data reported in this paper will be shared by the [lead contact](#) upon request.
- This paper does not report original code.
- Any additional information required to reanalyze the data reported in this paper is available from the [lead contact](#) upon request.

**EXPERIMENTAL MODEL AND STUDY PARTICIPANT DETAILS****Cell culture**

UC-MSCs were isolated from umbilical cord tissues obtained from the Zhujiang Hospital of Southern Medical University. Written informed consent was obtained from the donors. All the participants were Han Chinese, aged below 35 years, absence of infectious diseases, gestational age over 35 weeks, regular prenatal examinations, and no conditions that impede placental health. The experiments of human umbilical cord mesenchymal stem cells were conducted according to the ethical and regulatory guidelines approved by the ethical committee of the Zhujiang Hospital of Southern Medical University (No. 2019-KY-015-02). UC-MSCs were isolated by using a tissue explant method and were

maintained in serum-free medium (AM-V Serum Free Medium, tbdscience, sc-82013-G) supplemented with 1% penicillin and streptomycin (Gibco).

### Animal experiments

Male C57BL/6J mice aged 6–8 weeks were purchased from Guangdong Slack Jingda Experimental Animal Co., Ltd. All animal experiments were approved by the ethical committee of the Zhujiang Hospital of Southern Medical University (No. LAEC-2023-136).

## METHOD DETAILS

### Isolation and identification of UC-MSCs

UC-MSCs were isolated by using a tissue explant method and expanded and cryopreserved as we previously described.<sup>30</sup> Briefly, arteries and veins were separated, and umbilical cord tissue was cut into small pieces of about 1–2 mm, then placed in a 25-cm<sup>2</sup> flask and cultured in serum-free medium (AM-V Serum Free Medium, tbdscience, sc-82013-G) supplemented with 1% penicillin and streptomycin (Gibco). The flask was put in a humidified atmosphere at 37°C with 5% CO<sub>2</sub>, and when cells migrated from the tissue, the medium was changed every 3 days. At 80–90% confluence, cells were harvested with 0.25% trypsin digestion and passaged at a ratio of 1:3.

To characterize the surface markers of UC-MSCs, Passage 3 UC-MSCs were harvested and diluted in 1 × 10<sup>6</sup> cells/ml, then incubated with the following antibodies: PE Mouse anti-Human CD105, PE Mouse Anti-Human CD90, APC Mouse anti-Human CD73, APC Mouse Anti-Human CD14, PE Mouse Anti-Human CD34, and PE Mouse Anti-Human HLA-DR. All antibodies were from BD Sciences. Cells were analyzed by using the CytoFLEX flow cytometer (Beckman).

According to the manufacturer's instructions, the adipogenic, osteogenic and neurogenic differentiation of UC-MSCs was performed by using the adipogenic differentiation kit (Stem cell Technologies), osteogenic differentiation kit (Stem cell Technologies) and neurogenic differentiation kit (Promocell), respectively. Cells were incubated in a humidified atmosphere at 37°C with 5% CO<sub>2</sub>. For adipogenic and osteogenic differentiation, the medium was changed every 3 days. After 21 days, the lipid vesicles were revealed by Oil-red O staining, and calcium deposition was evaluated by alizarin red staining. For neurogenic differentiation, the medium was changed every 2 days. After 5 days, Nissl bodies were evaluated by Nissl staining.

### Hepatocyte differentiation from UC-MSCs

Hepatocytes were differentiated as described,<sup>53</sup> with some modifications. The differentiation process was divided into three stages: pretreatment step, differentiation step and maturation step. Passage 2–Passage 8 UC-MSCs were seeded at 4 × 10<sup>3</sup> cells/cm<sup>2</sup> in six-well plates in serum-free medium. Culture medium was switched 24 h later to pretreatment medium based on the serum-free medium supplemented with 20 ng/ml epidermal growth factor (Peprotech), 100 ng/ml activin A (Novoprotein) and 10 ng/ml fibroblast growth factor 4 (Peprotech) for 3 days. Thereafter, differentiation was induced by treating UC-MSCs with serum-free medium containing 20 ng/ml hepatocyte growth factor (Peprotech), 10 ng/ml fibroblast growth factor 4, 0.61 g/L nicotinamide (Sigma), 1% dimethyl sulfoxide (MP Biomedicals), and 1% insulin-transferrin-selenium (Gibco) for 10 days. Then cells were incubated with maturation medium containing 20 ng/ml oncostatin M (Peprotech), 1 μmol/L dexamethasone (Sigma), 1% dimethyl sulfoxide and 1% insulin-transferrin-selenium for 15 days. Medium was changed every 3 days.

### Treatment of differentiated cells with Sch B

Sch B (CAS #61281-37-6) was purchased from MedChemExpress, with purity 99.86%, molecular weight 400.46, and molecular formula C<sub>23</sub>H<sub>28</sub>O<sub>6</sub>. To examine the cytotoxicity of Sch B, 1 × 10<sup>4</sup> cells were seeded in 96-well culture plates in culture medium for 24 h, then the culture medium was switched to medium containing 0, 1, 10, 25, 50, 100, 200 μM Sch B, and cells were cultured in a humidified atmosphere at 37°C with 5% CO<sub>2</sub> for 72 h. The effects of Sch B on cell viability were qualified by using the Cell Counting Kit-8 (CCK-8; ApexBio Technology LLC).

Cytotoxicity test results allowed for determining the appropriate concentration of Sch B. To investigate the optimal treatment concentration and duration of Sch B, different concentrations were added at different stages of the induction process. QPCR was used to assess the expression of hepatic marker genes to evaluate the effect of Sch B.

### Quantitative real-time PCR analysis

Total RNA was extracted from cells by the Trizol method. cDNA synthesis was performed with 1 μg RNA with *M-MLV* reverse transcriptase (Accurate Biology) according to the manufacturer's instructions. Quantitative RT-PCR analysis was performed with the SYBR Green Premix *Pro Taq HS* qPCR Kit (Accurate Biology) and the Bio-Rad CFX Connect PCR detection system (Bio-Rad). The thermocycling parameters were 95°C for 30 sec, followed by 40 cycles at 95°C for 5 sec and 60°C for 30 sec. Primers used in this study are in [Table S1](#). The relative expression levels were analyzed by using the 2<sup>-ΔΔCt</sup> method. The mRNA expression levels were normalized with GAPDH.

### Immunofluorescence staining

Immunofluorescence staining was used to visualize hepatocyte-specific markers. Briefly, differentiated cells were fixed with 4% paraformaldehyde for 30 min, followed by permeabilization with 0.2% Triton X-100 for 30 min, then blocked with 3% bovine serum albumin for 1 h at room temperature. Subsequently, cells were incubated at 4°C overnight with Anti-alpha 1 Fetoprotein (AFP) (1:250; Abcam), Anti-Cytokeratin 18 (CK18) (1:400; Abcam), CYP3A4 antibody (1:500; GeneTex), Anti-Albumin (ALB) (1:500; Abcam), and hepatocyte nuclear factor-4α (HNF4α)

(1:250; Abcam) antibodies. Then next day, cells were incubated for 2 h at room temperature with respective Alexa Fluor conjugated secondary antibodies. Nuclei were stained with 4',6-diamidino-2-phenylindole (DAPI) for 10 min and observed under a fluorescence microscope (Zeiss).

### Albumin assay

At the endpoint of the differentiation process, cells were washed with PBS and incubated for 24 h with serum-free medium. The supernatant was collected to measure ALB secretion by using a human albumin ELISA kit (Mlbio) according to the manufacturer's protocol. The amount of albumin released was normalized to the total number of cells determined from each sample.

### Urea production

At the endpoint of the differentiation process, cells were washed with PBS and incubated for 24 h with serum-free medium supplemented with 3 mM NH<sub>4</sub>Cl. The supernatants were collected to analyze urea secretion with the human urea ELISA kit (Mlbio) according to the manufacturer's instructions. The amount of urea released was normalized to the total number of cells determined from each sample.

### Periodic acid-Schiff staining

Characterization for the glycogen storage potential was by the periodic acid-Schiff (PAS) staining system (Solarbio). Briefly, after 28 days of differentiation, cells were fixed with 4% paraformaldehyde for 30 min, then incubated with periodic acid solution for 5 min, washed three times with PBS and incubated in Schiff reagent for 15 min. Finally, cells were counterstained in hematoxylin solution for 1 min and observed under a microscope.

### Transcriptome sequencing

After 28 days of differentiation, total RNA was extracted from cells by using the RNeasy Plus Mini Kit (Qiagen). The sequencing data was provided by Shanghai Genechem Co. RNA quantity and integrity were verified by using the Agilent 2100 Bioanalyzer. The RNA-seq library was prepared with the NEBNext Ultra RNA Library Prep Kit for Illumina according to the protocol provided by the manufacturer. The library was assessed by using the Agilent 2100 Bioanalyzer. Finally, sequencing was performed on an Illumina HiSeq sequencer with a 150-bp paired-end sequencing reaction. Primary sequencing data from Illumina HiSeq sequencing were referred for raw read quality control. The clean reads obtained were used for downstream bioinformatics analysis. Then the clean reads were aligned to the reference sequences by using HISAT2 software. The expression levels of genes were determined according to the value of fragments per kilo bases per million fragments (FPKM). We then used DESeq R package to filter differentially expressed genes (DEGs). After statistical analysis, we screened DEGs as follows:  $|\log_2\text{foldchange}| > 1$ , with  $p < 0.05$ .

### Gene ontology (GO) and KEGG enrichment analysis

The Gene Ontology (GO) database (<http://www.geneontology.org/>) was used to determine GO terms for DEGs. The Kyoto Encyclopedia of Genes and Genomes (KEGG) database (<http://www.kegg.jp/>) was used for pathway enrichment analysis of DEGs. Then, Fisher's exact test was used to identify significantly enriched GO terms and significant enrichment pathways of DEGs. The false discovery rate was used to correct p values, with  $p < 0.05$  considered statistically significant.

### Western blot analysis

Differentiated cells were harvested and lysed in RIPA buffer supplemented with proteinase inhibitor cocktail (MedChemExpress). Proteins were separated on 10% SDS-PAGE gel and electro-transferred to PVDF membranes (Millipore). The membranes were blocked in blocking solution (5% skim milk in PBS) for 1 h at room temperature, and incubated overnight at 4°C with primary antibodies against JAK2 (1:1000, Cell Signaling Technology), p-JAK2 (Tyr1007/1008, 1:1000, Abcam), STAT3 (1:2000, Cell Signaling Technology), p-STAT3 (Tyr705, 1:2000, Abcam), HIF-1a (1:500, Santa Cruz Biotechnology), cyclin D1 (1:5000, proteintech), c-Myc (1:1000, Abmart), GAPDH (1:2000, Affinity) and  $\beta$ -actin (1:3000, Affinity). Thereafter, the membranes were incubated at room temperature for 1 h with horseradish peroxidase-linked secondary antibodies (1:2000, Wanleibio). The protein bands were detected by using an enhanced chemiluminescence kit (Wanleibio).

### Preparation of GelMA hydrogel and biocompatibility assay

Photoinitiator lithium phenyl-2,4,6-trimethylbenzoyl phosphine (LAP) (Engineering for Life) standard solution with a concentration of 0.25% was prepared according to the manufacturer's instructions. GelMA (Engineering for Life) was reconstituted at 10% (w/v) in the LAP standard solution and incubated in a 65°C water bath until completely dissolved. The GelMA solution was subsequently sterilized using a 0.22  $\mu\text{m}$  filter.

To evaluate the biocompatibility of the GelMA hydrogel, cells were fully mixed with the GelMA solution and added to a 24-well plate. The GelMA-cell suspensions were cross-linked into hydrogels by the UV light (405 nm) in 15 seconds and growth medium was added. The Live/Dead staining was performed to assess cell viability according to the manufacturer's instructions (Live/Dead Assay Kit, KeyGEN BioTECH) at days 1, 3, and 7.

### Establishment and treatment of chronic liver fibrosis model

To induce liver fibrosis, we administered 1 ml/kg of CCL<sub>4</sub> or vehicle olive oil intraperitoneally twice a week for 6 weeks to C57BL/6J mice aged 6–8 weeks. The mice were divided into five groups: Control group (n = 5); CCL<sub>4</sub> group (n = 10); UC-MSCs group (n = 10) which received transplantation of undifferentiated UC-MSCs; Sch B(–) group (n = 10) which received transplantation without Sch B-induced HLCs; Sch B(+) group (n = 10) which received transplantation with Sch B-induced HLCs.

The mice were positioned in a supine position and prepared under anesthesia. Following sterilization, a midline abdominal incision was performed to expose the liver. 100  $\mu$ l GelMA hydrogel containing  $5 \times 10^5$  cells was injected onto the liver surface and immediately irradiated with UV light (405 nm) for 15 seconds to solidify and attach to the liver surface. Then the surgical wound was closed in layers with a routine method.

### Biochemical assay and histological analysis

After 7 and 14 days after transplantation, the mice were sacrificed to collect liver tissues and serum. Serum alanine aminotransferase (ALT) and aspartate aminotransferase (AST) were assessed by automatic biochemical analyzer (FUJIFILM). Human albumin in mice liver tissues was detected and quantified using the human albumin ELISA kit (Neobioscience) according to the manufacturer's instructions. Liver tissues were fixed with 4% paraformaldehyde, embedded in paraffin, and sectioned at 4  $\mu$ m. The sections were dewaxed and rehydrated, and stained with HE. The fibrotic area was stained with a Masson trichrome staining kit (ZSGB-BIO) and a Sirius Red Stain Kit (Solarbio) following the manufacturer's instructions. Image J software was employed to quantify the area of collagen positivity. For immunohistochemistry staining, sections were incubated overnight with primary antibody against CD31 (1:500, Cell Signaling Technology) at 4°C. Thereafter, the sections were incubated with horseradish peroxidase-conjugated goat anti-mouse secondary antibody (1:200, Wanleibio) followed by visualization with 3,3'-diaminobenzidine tetrahydrochloride (DAB, ZSGB-BIO). Finally, the sections were stained with hematoxylin. Slides were scanned using Panoramic scanner (3D Hitech Ltd.) and analyzed using SlideViewer software (3D Hitech Ltd.)

### QUANTIFICATION AND STATISTICAL ANALYSIS

Statistical analysis was performed using GraphPad Prism 8.0 or SPSS 20.0. Group comparisons were performed using an unpaired Student's t test and one-way ANOVA. The data were presented as mean  $\pm$  standard deviation (SD) from at least three independent experiments.  $p < 0.05$  was considered statistically significant.